Drop size distributions in stirred liquid/liquid systems
Influence of the dispersed phase

Master final project

Giulia Carlucci
Matr. Nr. 331007

Technische Universität Berlin
Fakultät III

Institut für Prozess- und Verfahrenstechnik

Fachgebiet Verfahrenstechnik

Prof. Dr.-Ing M. Kraume

Betreuer: Dipl.-Ing S. Hermann

Technische Universität Berlin

FACULTY III

School of Process Sciences and Engineering

Department of Process Engineering

Chair of Chemical and Process Engineering

Professor Dr.-Ing. M. Kraume

Project Definition

for

Giulia Carlucci
Matr. No. 331007

Title: Drop size distributions in stirred liquid/liquid systems - Influence of the dispersed phase

Definition: Stirred liquid/liquid systems are of great importance in the chemical, food, and pharmaceutical industries. The Drop Size Distribution (DSD), which results from the opposed phenomena of drop breakage and coalescence, plays a major role in such processes. It determines the interfacial area i.e. for heat or mass transfer processes.
Process and geometrical parameters, but also physical properties of the dispersed phase influence the occurring DSD. For scale up issues it is important to do experimental investigations in lab, as well as in larger scales.
The aim of the project is to find a low-viscosity oil as a model substance, which can be employed as the dispersed phase for larger scale investigations. Therefore, different oils should be chosen, considering cost and security aspects, as well as physical parameters. The properties of these oils should be similar to those of toluene, which is normally used for lab-scale investigations. To investigate the occurring DSD, endoscope measurements should be conducted. A software for automated image analysis should be tested for suitability by comparison with manually determined DSD. Additionally a laser-based probe (Inline Particle Probe – IPP30), which provides online information about the drop size distributions, should be applied.
The results of the experimental investigation have to be documented, validated with regards to reproducibility and accuracy, and discussed. Literature research is an integral part of the thesis.
The work has been performed following the safety instruction for laboratories. All security guidelines and operation instructions for the Chair of Chemical and Process Engineering have to be fulfilled.

Release date: 1/3/2010
Closing date: 26/8/2010

Supervisor: Dipl.-Ing. Stephanie Hermann
Prof. Dr.-Ing. Matthias Kraume

Prof. Dr.-Ing. M. Kraume

I Preface

I swear on my honour the originality and independence on the creation of this text. I would like also to thank to all the people who helped me along the way and to Berlin which makes dreams come true.

Berlin,
August 26, 2010

_____

Giulia Carlucci

Index

I. Preface I

II Index II

III Notation and abbreviations III

1. Introduction 1

2. Theoretical part 3

2.1. Stirred liquid/liquid systems 3

2.2. Parameters influencing drop size distribution 10

2.3. Measurement techniques 13

3. Material and methods 15

3.1. Experimental set up and procedure 13

3.2. Analysis of drop size distribution 15

3.3. Model systems 19

3.4. Measurment of physical properties 20

4. Results and discussion 20

4.1. Physical properties of the different oils 24

4.2. Investigation inthe stirred tank 24

5. Conclusions 28

6. Bibliography 31

7. Annex..... 35

Notation and abbreviations

Latin letters

d_{32}	[m]	Sauter mean diameter
d_{max}	[m]	maximum stable drop diameter
Re	[-]	Reynolds number
We	[-]	Weber number
N'_{vi}	[-]	viscosity group
N_{we}	[-]	generalised Weber group
E_{kin}	[J]	kinetic energy
E_{γ}	[J]	interfacial energy
$\overline{w'^2}$	[m/s]	mean turbulent fluctuating velocity
$d_{p,max}$	[m]	maximum stable drop diameter
D	[m]	impeller diameter
n	[-]	refrax index
T	[m]	stirred tank diameter
V	[ml]	stirred tank volume
$d_{I,B}$	[m]	baffles dimension
H	[m]	solution dimensioning in the tank
h	[m]	distance tank bottom-stirrer
Δp	[Pa]	pressure difference
R_1	[m]	radii of curvature drop phase
R_2	[m]	radii of curvature surrounding phase
F	[s]	fall time
K	[-]	sphere constant
S_{sph}	[kg/m^3]	sphere density
S_{liq}	[kg/m^3]	liquid density
d_{sph}	[m]	sphere diamenter
m_{sph}	[kg]	sphere mass

t	[s]	time
h	[m]	stirrer blade height
d	[m]	drop diameter

Greek letters

σ	[N/m]	surface tension
γ	[N/m]	interfacial facial tension
φ	[-]	dispersed-phase volume fraction
ν_{cyn}	[mm²/s]	kinematic viscosity
ν_{dyn}	[P	dinamic viscosity
Λ	[m]	macro lenght scale
λ	[m]	micro lenght scale
ε	[J]	dissipation energy
ρ	[kg/m^3]	density

Abbreviations

DSD	drop size distribution
IPP-30	in-line particle probe-model 30
BC	Boubble Count
DD	Drop Dead
SFT	surface t nsio
IFT	interfacial facial tension
UP	ultra purified
DW	deionized water

Subscripts

d	dispersed phase
max	maximun
w	water
sph	sphere

kin	kinematic
dyn	dynamic
rel	relative
liq	liquid
tol	toluene

1. Introduction

The growing importance of dispersed systems in numerous chemical engineering processes led to close examinations on the behaviour of such systems.

In chemical, pharmaceutical, mining, petroleum and food industries, the mixing of two immiscible liquids in turbulent flow is a common operation.

The size distribution of the droplets plays an essential role in the overall performance of these processes.

In stirred tanks the mass transfer rate between the phases in liquid-liquid systems does not only depend on the dynamics of the motion between the two immiscible liquids.

Much more dependence is given from the particle size distribution of the drops.

It is well known, that geometrical and process parameters, as well as the used system influences the drop size distributions. Although numerous investigations have been conducted, the prediction of the drop size distribution under the influence of the mentioned parameters is still inaccurate. Therefore expensive experimental investigations are still needed for the design of new reactors.

This work was conducted during the project “Modelling, Simulation, and Control of Drop Size Distribution in stirred liquid/liquid systems”. The aim of this project is the model-based control of drop size distributions in stirred systems.

Therefore different investigations are needed, including experiments in different scales.

A commonly used dispersed phase for investigations of liquid/liquid systems, expecially related to extraction processes, is toluene. Due to these solvent properties the study of the system with optical measurement devices is possible. However, because of the dangerous properties of toluene, it is important to find alternatives and more safety solvents.

Therefore the aim of this work was to find a substitute dispersed phase. Cost and security aspects, as well as the physical parameters should be considered.

After choosing different oils, the physical properties were measured and investigations in the stirred reactor conducted. Bearing in mind that the main reason for which toluene is not the best choice as a research solvent is its high flammability, the solvents choosen have no flammability risk at all.

An endoscope was choosen to measure the drop size distribution. In addition another device was used: an Inline Particle Probe (IPP-30).

Pictures, taken by endocope were analyzed manually with the support of a program called Bubble Count (BC) and automatically with a program called DropDead (DD).

2. Theoretical part

2.1. Stirred liquid/liquid systems

Liquid-liquid dispersions have been the subject of many studies dealing with mass transfer for industrial processes such as solvent extraction, emulsification and multiphase reactions.

In a liquid-liquid system, before agitation starts, the dispersed organic phase is completely separated from the aqueous one. When the agitation of the stirrer starts the energy input disperses the organic phase into the aqueous one (Espejo, 2008) as it can be seen in Fig.1.

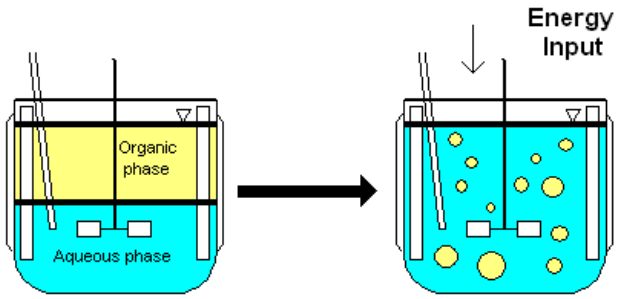

Fig.1 : Behaviour of a liquid/liquid system before and under agitated conditions (Espejo 2008)

The drop size distribution of the dispersed phase results from the revese phenomena of drop breakage and coalescence (Fig.2) .The DSD plays an essential role in the overall performance of many industrial processes.

Infact in stirred tanks the mass transfer rate between the phases in liquid-liquid systems does not only depend on the dynamics of the motion between the two immiscible liquids, but much more on the drop size distribution of the drops (Maaß et al., 2006).

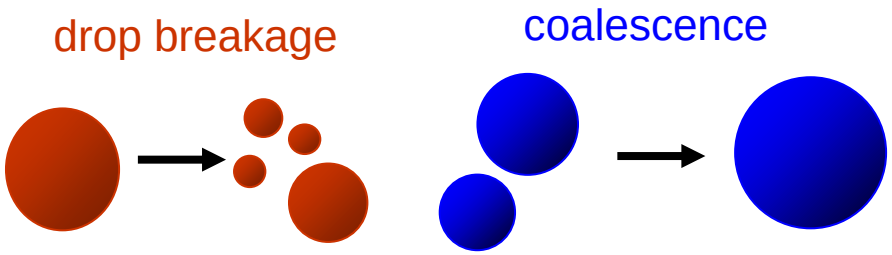

Fig.2 : Representation of drop breakage and coalescence (Espejo, 2008)

If the Reynolds number in mixing vessel is greater than 10^4 the flow become turbulent (Kraume et al., 2004). Eddies are formed in the continuous phase and some of them break the droplets when they collid with each other.

The largest eddies are in the order of the stirrer blade height and are characterized with the macro-lenght scale Λ.

This large eddies turn into smaller ones, as represented in the Fig.3 (Lutz, 2008).

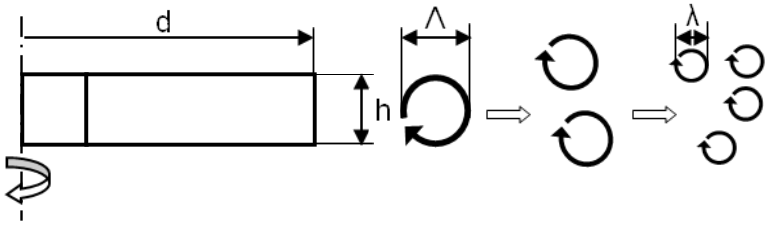

Fig.3 : Vortex decay because of a turbulent flow (Lutz, 2008)

The smallest eddies of the system are characterized by the fact that they can only transform their mechanical energy into heat because of viscous forces (Kraume et al., 2003). They are characterized by the microscale λ (Kolmogrov lenght) which depend on the kinematic viscosity and the dissipation energy (Kolmogrov, 1941).

$$\lambda \approx h \tag{1}$$

$$\lambda = \left(\frac{\nu_{kin}^3}{\varepsilon_m} \right)^{1/4} \tag{2}$$

As mentioned above, the DSD produced in a mixer is the results of two reverse phenomena:

-Drop breakage, due to the turbulent field

-Coalescence which depends on the collision frequency and the coalescence efficienty between drops.

The higer the dispersed phase fraction, the more often collision between droplets occur.

Fig.4 schematically describes the main steps of two coalescing drops, according to Chesters (1991).

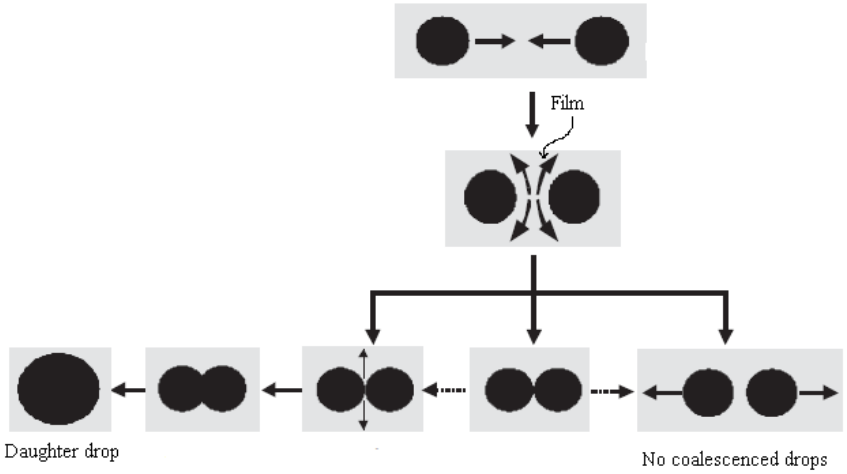

Fig.4 : Coalescence steps (Schuchmann and Danner, 2004)

Two drops, with their relative velocity, approach to each other.

They touch themselves, deform their shape and between them a film of the surrounding phase is generated. This film reachese a critical thickness and tears.

The completly film tear is the last step of drops coalescence that generates a new drop. If the time of contact of two droplets is less than the duration of the film drainage, or the film does not fall below its critical thickness, there is no coalescence.

Below are reported equations that are the mathematical basis for the description of interactions between turbulents fluid-flow and the size characteristics leading to the most often used equation for the Sauter diameter.
The theoretical concept was carried out by Hinze (1955) and Shinnar (1961).

The Weber number is one of the most important indicator of the breakage condition of a drop and the resulting daughter drop sizes. It represents the ratio between the kinetic energy E_{kin} and the surface energy E_{γ} ,which means the ratio of the external deforming forces to the stabilizing surface forces.

$$We_{,d_{P,\max}} = \frac{E_{kin}}{E_{\gamma}} = \frac{\rho \cdot \overline{w'^2} \cdot d_{P,\max}}{\gamma} \tag{3}$$

Were ρ is the density, $\overline{w'^2}$ is the mean turbulent fluctuating velocity , $d_{P,\max}$ is the maximum stable drop diameter and γ is the interfacial tension.

Under the condition that the energy dissipation rates in the stirred tank are spatially uniform Eq. 3 results in an equation for the maximum drop diameter:

$$\frac{d_{P,\max}}{D} = C_1 \frac{N^2 D^3 \rho}{\gamma} = C_1 \cdot We^{-0,6} \tag{4}$$

Were N is the stirrer rotation speed, D is the stirrer diameter and C_1 is a constant factor. This maximum drop diameter can be correlated linearly with the Sauter diameter d_{32}.

$$\frac{d_{32}}{D} = C_2 \cdot We^{-0,6} \tag{5}$$

Normally, occuring coalescence processes are taken into account by a modification of Eq. 5. Most published correlations for d_{32} extend Eq. 5 by the expression $C_4(1+C_3\varphi)$.

$$\frac{d_{32}}{D} = C_4(1 + C_3)We^{-0,6} \tag{6}$$

C_4 depends on the impeller type whereas C_3 depends on the coalescence tendency.

Systems that coalesce easily have high values of C_3 and those that coalesce slowly have low ones. Values for C_3 from about 3 to about 20 have been reported by Pacek et al. (1994) and Kraume et al. (2004).

At a constant dispersed phase fraction φ Eq. 6 shows that the Sauter diameter depends only on the power input per unit mass. A further dependency on the geometrical size of the apparatus should not exist.

Therefore, the exponent -0,6 of the Weber number in relation to d_{32} is of great importance for scale up.

In a second model Shinnar (1961) derived an equation for the minimum drop diameter resulting from turbulent fluctations and adhesion forces. Thereby, the effect of coalescence is taken into account. The following proportionality has been deduced for systems dominated by coalescence:

$$\frac{d_{32}}{D} = C_5 We^{-0,375} \tag{7}$$

Different authors estimated different exponent which are for instance summarized by Kraume et al. (2004): Kipke (1981), as well as Brooks (1979) estimated an exponent of -0,3 whereas Hartland et al.(1987) found -0,4 and Nienow et al.(1998) -0,4. On the other hand experimental results for a diluite system from Maldyga and Bourne (1993) led to an exponent of -0,9.

Hinze (1955) established a basis for data correlation using dimensionless numbers, when both surface and dispersed-phase viscous forces contribute to drop stability in a region far away from the impeller. He proposed that two independent dimensionless groups, both based on drop diameter, were required and chose them to be the viscosity group, N'_{vi} wich represent the ratio of dispersed-phase viscous energy to surface energy and the generalized Weber group, N_{we}, which is defined as follows:

$$N_{we} = \gamma \cdot d / \sigma \tag{8}$$

$$N'_{vi} = \frac{\eta_d}{\sqrt{\rho_d \cdot \sigma \cdot d}} \tag{9}$$

2.2. Parameters influencing DSD

It is well known, that geometrical, as well process parameters and physical properties of the system influence the occurring DSD. Therefore many research studies have been conducted to determine and describe these influences.

Comprehensive studies dealing with the influence of energy input, temperature, ionic strenght, pH or dispersed phase fraction, therefore exist. In this chapter, the influence of some of these parameters should now be depicted

pH-value

The coalescence behaviour is particulary influenced by pH. Different methods for changing coalescence behaviour are known in literature, e.g. using very diluite systems to make collisions of droplets improbable or adding surfactants to immobilize the droplet surface. Indeed the very diluite systems are technically not relevant and the surfactants may dominate and change the

behaviour of liquid-liquid dispersion drastically e.g causing local differences of the interfacial tension and deform droplets.

Gäbler et al. (2006) focused on changing the coalescence behaviour by increasing the pH-value and thereby the droplet charge.

From the results of their experiments, made in a baffled-glass vessel with toluene as dispersed phase (φ =5-50%), and stirrer speed between 400 and 700 rpm is highlighted that pH has got a great influence on the transient evolution, as well as on the steady-state distribution of the drop.

Infact with higher pH, coalescence is hindered considerably. As a conseguence, the transient evolution of DSD after starting the stirrer changed and the time for reaching the stationar distribution increase. The autors noticed that, in agreement with Skelland and Kandel (1992) and Hong and Lee (1985), who reported transient response occurring within less than a second, steady state was reached for lower pH within 1 min. For pH 11 and 13 they founded a change of DSD and Sauter diameter up to 30 min, a time scale observed also in other researches.

Viscosity

It's known from force-balances that drop are stabilized in agitated liquid-liquid systems by surface and dispersed-phase viscous forces and are broken by forces associated with the continuous-phase turbulence (Calabrese et al, 1986).

The datas from literature demostrate that dispersed-phase viscosity has a profound influence on both the mean drop size and the DSD: Calabrese et al. (1986) analysed the influence of the dispersed-phase viscosity on the DSD at constant interfacial tension for diluite suspension by disperding silicone oils of various grades in water.

This research were made with silicone oils (Dow Corning oil 200 Fluid) with viscosity in a range between 10^2 and 10^4 mPas, and interfacial tension around 10^{-2} N/m. The concentration of the dispersed phase was kept less than φ =0,15%.

It was noticed that at constant conditions of agitation, the steady-state drop size distribution enlarge considerably as dispersed phase viscosity ν_d increases. The size of the smallest drops decrease while their number increases; as well as

the size of the largest drops increase while their number decreases and the DSD gets wider.

In a work carried out by EL-Hamouz et al (2009), it was found that the We exponent of the theoretically derived correlation $d_{32} \approx We^{-0.6}$, which is valid for a low-phase fraction φ (0.01), was found to vary around 0.4 with increasing the dispersed-phase viscosity ν_d. This is due to the complex breakage-coalescence mechanism.

Dispersed phase fraction

Coalescence, dispersion processes, and settling are all affected by the dispersed-phase concentration, e.g., coalescence rates increase with increasing φ.This is due to both an increase collision frequency and rheologically changes that enable longer contact intervals to be obtained.

El-Hamouz et al. (2009) noticed that the high disperse phase concentration also affect small scale turbulent eddies, reducing their intensity and making them less able to disperse drops.

They carried a set of experiments with a silicone oil (Dow Corining Oil 200 Fluid) in order to measure the drop size distribution and d32 of emulsion of various dispersed-phase viscosity grades at different values of φ.

They concluded that there is a very weak dependence of the equilibrium d_{32} on φ but a high-dispersed phase concentration affect small scale turbulent eddies, reducing their intensity and making them less able to disperse drops. As a conseguence of it the breackage decrease and the Sauter diameter increase, as Fig.5 shows.

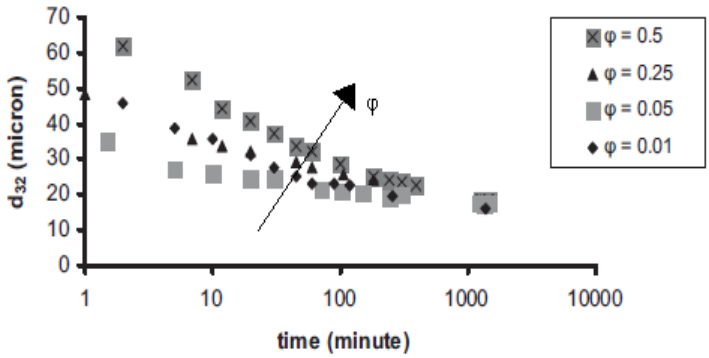

Fig. 5 : Sauter diametere for different phase fractions, with high viscosity silicone oil (El-Hamouz et al (2009))

2.3. Measurement techniques

To measure drop size distributions in stirred liquid/liquid–systems, there are many different measurement techniques avaible on the market. They are based on different physical properties and described in literature (Maaβ et al., 2010; Wang et al., 2006; Mondal et al., 2010).

To investigate stirred liquid/liquid systems is important to use in-line measurement techniques with the device inside the system.

This is due to the fact that the dispersion is fast coalescening and with external sampling the results would be totally different.

The endoscope was choosen by many autors because it is the most reliability device for taking pictures of the dispersed phase (Maaß et al., 2010; Pacek et al., 1994).

Infact many different approaches and techniques have been published but, according to them, the endoscope is the device that provides the most exact results even with high volumetric volume fraction until $\varphi \leq 50\%$.

Other in-line devices, like laser ones, e.g. 2D ORM®, FBRM®, gave unresonable results concerning size analysis and the change of the size over the time (Maaß et al., 2010).

Using the endoscope images are taken intrusively from inside the reactor by placing it in front of a CCD camera as a microscope lens.

This measurement technique provides quantitative good results but needs a long time to analyze the images and to compute the DSD as well as the Sauter mean diameter.

An example of the sharpness of the endoscope images is showned in Fig.6:

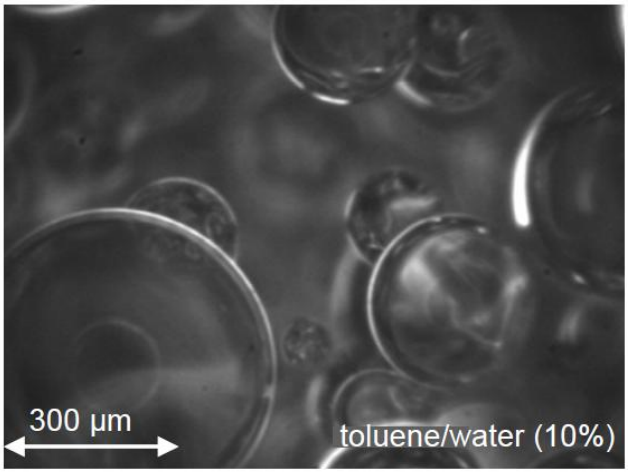

Fig. 6: Example of photo of the system toluene and water, pH 7, 475 rpm, 10% dispersed phase fraction (Maaβ et al., 2010)

According to Kraume et al. (2004), normally 200 images have to be taken for each speed and time, in order to count at least 300 droplets to achieve a reliable distribution.

3. Material and methods

3.1. Experimental set up and procedure

To investigate the drop size distribution in stirred liquid/liquid-systems the set up, depicted in Fig.6 was used. It consists of the baffled batch reactor, the stainless steel stirrer, the IPP-30 and the endoscope.

The experiments were carried out in a baffled-glass vessel. The dimensions, referring to the scheme in Fig. 7, are depicted in Tab. 1.

Tab. 1 : Stirred tank dimensions and characteristics

T	H	$d_{I,B}$	w_B	h	D
150 mm	T	0,8 T	0,08 T	0,33 T	0,33 T

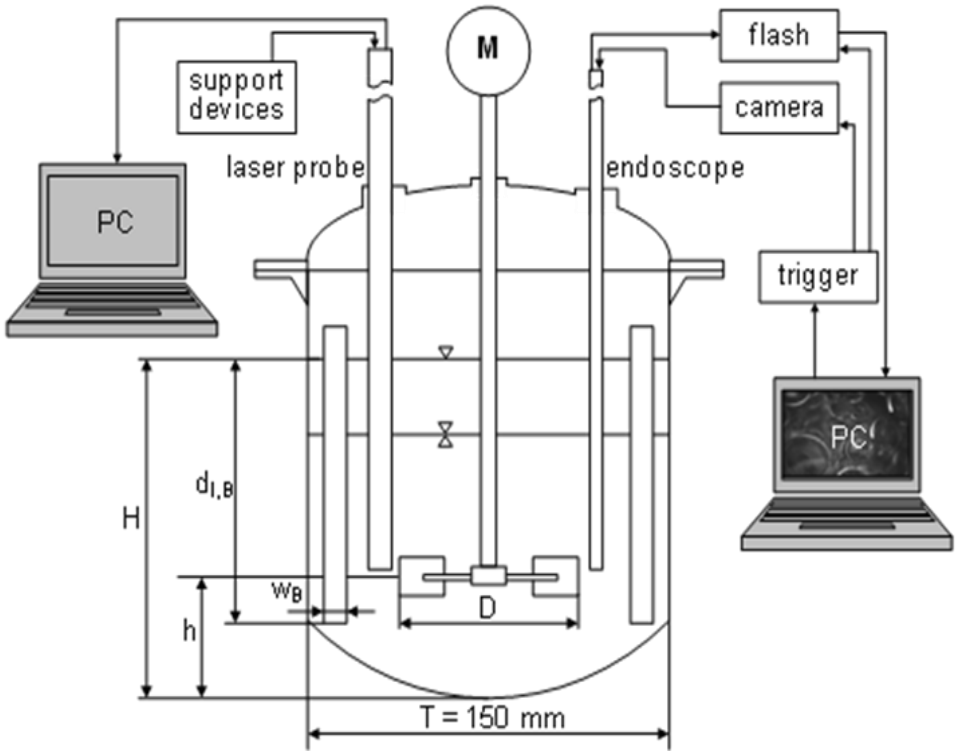

Fig. 7: Workbench arrangement

After cleaning the tank, the stirrer and the measurement devices with purified water and acetone, in order to remove impuritie, the workbench was prepared.

The stirrer was connected to the Rushton turbine and positioned 50 mm from the bottom of the vessel. Purified water, where some droplets of KOH were added to adjust the pH-value to 7, and the dispersed phase were added.

The IPP-30 and the endoscope were positionated in line with the stirrer so the flow passes the devices orthogonal and going through them.

The temperature was fixed to 20°C, by refrigeration.

For every solvent three different stirrer speeds were used. They were applied for one hour.

After the higest stirrer speed experiment, the speed was decreased until the lowest speed in order to study the coalescence behaviour (Tab.2).

For the lowest stirrer speed, it had to be ensured, that there was no more visible phase separation. Therefore the lowest stirrer speed was differing for the different oils

According to the behavior of each dispersed phase, the first experiments were made with a stirrer speed of 475 rpm instead of 400 rpm if there were no complete phase dispersion at such low speed, after 5 minutes.

Tab. 2 : Experiments set up

Dispersed phase	**N [rpm]**
Toluene	400-550-700
Fauth paraffin oil FC1013	400-550-700
Fauth paraffin oil FC2006	475-550-700-475
Roth Silicones silicon oil -M3	475-550-700-475
Wacker Silicones dimethicone	475-550-700
Mobil velocite oil 3 system	550-700
Roth Silicones silicon oil-M3 with mirror	475-550-700-475

Between each experiment, except for the last ones made in order to study the coalescence behaviour, the system was let stand untill there was again complete phase division.

3.2. Analysis of drop size distribution

The measure of the drop size distribution in liquid-liquid dispersions is still a challenging task as only few measure devices exist.

As mentioned above, in this work an in situ endoscope technique (Fig. 8) was installed: images were tacken placing a 7 mm thick endoscope in front of a CCD camera.

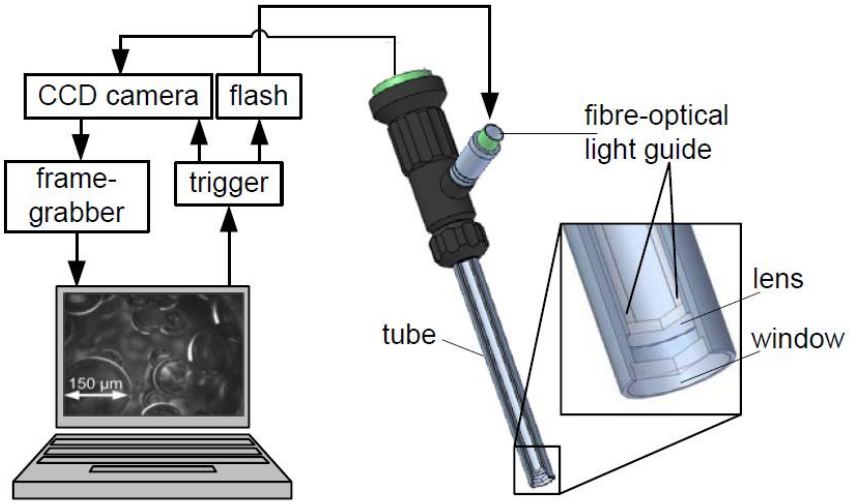

Fig. 8: Endoscope device (Maaβ et al., 2010)

After preparing the experiment, the stirrer was turned on and the endoscope parameters were manually set up according to the feature of images taken for each solvent (see Annex, Tab A.1). This setting is very important because images taken with the endoscope should be as sharp as possible, in order to use them not only with a manual counting program, called Boubble Count (BC), which takes almost 45 minuts for a serie of 200 picures, but also with an automatical counting program, called Drop Dead (DD).

For DD the border line is the quality of images taken by the endoscope, when the optical quality of the pictures is good enough, an automatical counting of more series of 200 pictures each gets possible.

After calibrating DD it was possible to let the program automatically count many series of images, referred to the same solvent with the same optical properties, at different speed and time steps.

In order to study the reliability of DD, the results obtained with DD were compared with the BC ones referred to the same serie. Some parameters in DD were rectified according to this comparison to create an improved model for the examinated solvent, which gave closer values of Sauter diameter and DSD in comparison to the manual counitng results.

After collecting the data for each solvent, at each stirrer speed, they were studied to achieve the DSD and the Sauter diameter.

Because one of the aims of this work was to study the suitability of DD, not all the time steps were manually counted: for each solvent the smallest and the biggest droplets were counted to see which kind of drops and how good DD recognizes them.

Four series of 200 images each, made with the endoscope, were manually counted. They were corresponding to the first and last time step: in this way it was possible to study the variation of the d_{32} with the time and with the stirrer speed increase.

Going through each picture, using Boubble Count (BC), the sharpest droplets were choosen and their cumulative probability was calculated, as well as the Sauter diamenter.

DD was calibrated, for the solvents, choosing one serie of images.

Becouse DD tends to recognize smaller droplets than by manual counting, the choosen serie to calibrate DD, was the one referred to the lowest velocity, after the first minute of experiment. That was the serie with the biggest drops.

The DD window is showned in Fig. 9.

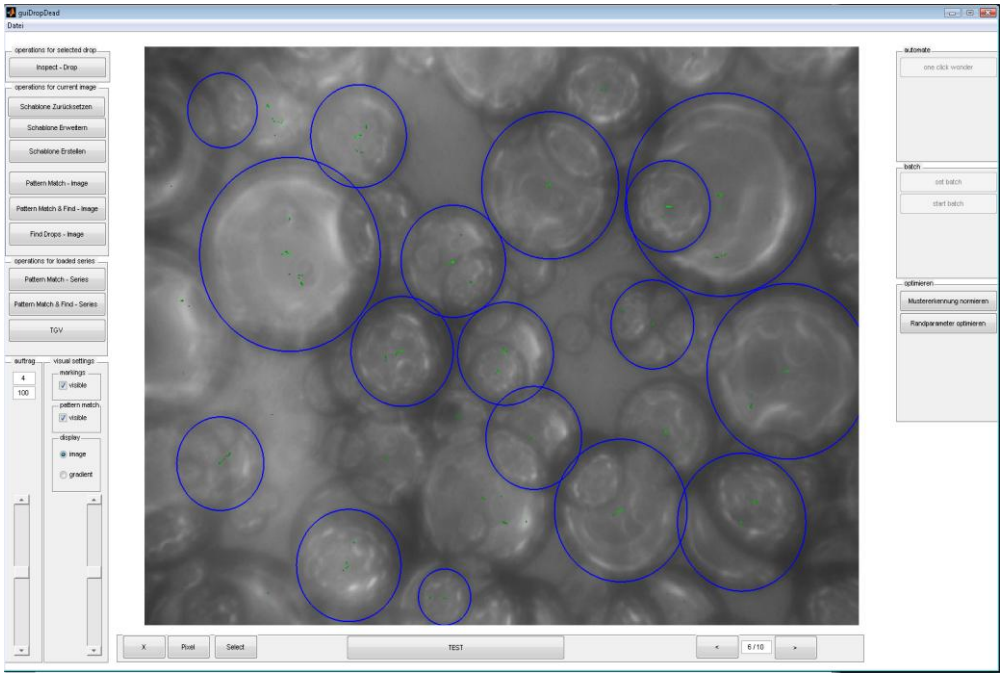

Fig. 9: DD window and automatical counted drops marked in blue

Moreover an IPP-30 (Fig.10) was used to record the distribution of droplets.

The Inline Particle Probe IPP 30 is based on a modified spatial filtering technique and allows the measurement of the transient drop size distribution online.

It is a method of determining the size and velocity of the drops simultaneously (Petrak et al., 2002).

The main principle of this technique is to observe the shadow of the drops moving through a small channel. When the particle passes through the fiber-optical probe an impulse is generated and the particle size thereby calculated.
A detailed physical description can be found in Petreak et al (2002).

The advantages of this in-line measuring device are the low hardware requirements and the robust design at reasonable investment costs.

The IPP 30 technique is avaible from PARSUM (Petrak 2002, Maaβ et al.2010).

The measurement value represents a chord lenght (Fig. 10); by accumulating results from individual particles the chord length and the velocity distribution are calculated.

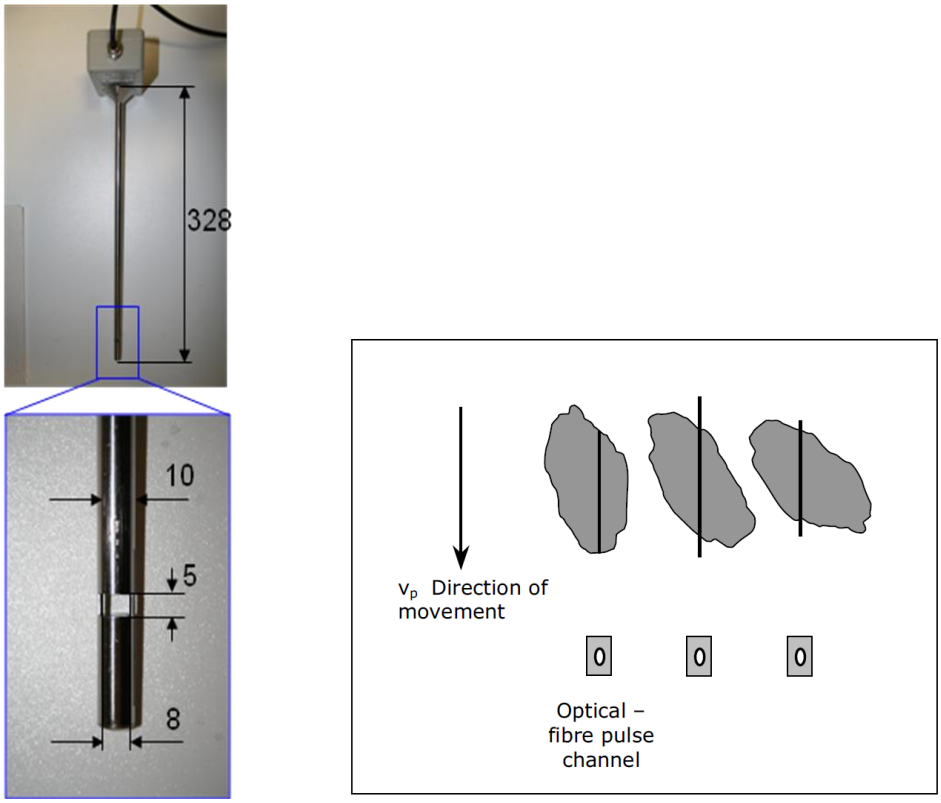

Fig. 10: Dimension of the IPP 30 device (left) and measured chord length (right)

The IPP-30 saves the particle size data in a ring buffer and the DSD is calculated online during the experiment.

The window on the IPP-30 connected computer (Fig. 11) shows the particle distribution in real time.

Additionally all particles in the ring buffer were saved after 1, 3, 5, 10, 15, 25, 40 and 60 minutes and, at the same time, 200 images with the endoscope were taken. As explained in Chapter 2.3, 200 is the minumum pictures number to achieve a reliable distribution.

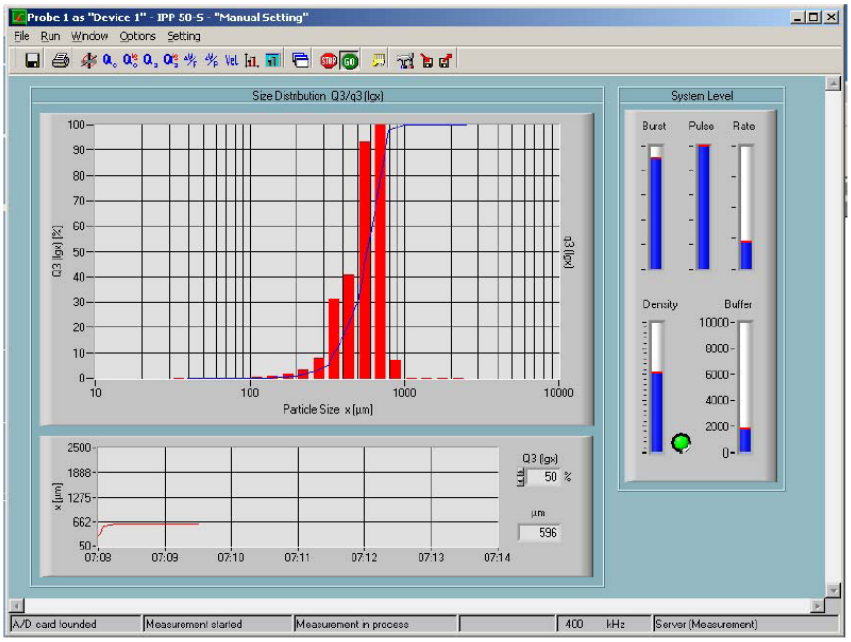

Fig. 11: Window for particle distribution $Q_3(x)$

3.3. Model systems

The system of the experiments consisted of purified water as a continuous phase and six different organic coumponds as the dispersed phase.

The pH-7 for the deionized water was guaranteed by adding some drops of a 3M KOH solution and checking with a pH-meter the accuracy of the value adjusted as standard.

No additional electrolytes were added.

In each experiment a different dispersed phase was used.

The solvent used to investigate liquid/liquid-systems as a standard is toluene (Misek et al., 1985). The other ones were choosen according to physical properties like viscosity, density, refrax index that should be similar to the ones of toluene.

In Tab. 3 the different tested oils, as well as their physical properties, given by the seller are listed.

Tab. 3: Dispersed phase properties

Name	Physical State	Cinematic Viscosity [mm²/s] (20°C)	Refrax Index (20°C)	Density [kg/m³] (15°C)	Solubility in water [g/l]	Danger	Price (€/l)
Toluene	Clear liquid	0,7	1,496	866	0,52	F+	18,99
Roth Silicones silicon oil -M3	Clear liquid	10	1,382	900	-	-	21,9
Wacker Silicones dimethicone	Clear liquid	5	1,382	920	-	-	8,08
Fauth paraffin oil FC1013	Clear liquid	1,6-2,15	1,418	740-760	-	-	5,95
Fauth paraffin oil FC2006	Clear liquid	9,5-16	1,4551	750-850	-	-	5,95
Mobil velocite oil 3 system	Clear liquid	2	1,4474-1,4476	802	-	-	3,18

3.4. Measurment of physical properties

Interfacial tension

The interfacial facial tension (IFT) is of great importance for the dispersed phase because it influences the drop stability and therefore the breakage of drops. The interfacial tension was measured by a pendand drop (Fig.12).

For each proof the solvent has been insuffled in a needle with a diameter of 0.5 mm. Droplets that were going out from the tip of the needle were photographed by a camera.

Picture were taken when droplets were as big as possible before falling down and also according to the focus-assistant values of sharpness given by the measure program.

An example of a pendand drop is given in Fig.12.

Fig.12 : Example of pendant drop

Setting the focus and the light was particulary important as well as a deep cleaning procedure of all the devices in order to eliminate all the impurities that strongly influence the results.

The operating principle of the device is the Young-Laplace function :

$$\Delta p = \gamma(\frac{1}{R_1} + \frac{1}{R_2}) \quad (9)$$

Where Δp is the pressure difference across the fluid interface, γ is the interfacial facial tension and R_1 and R_2 are the principal radii of curvature (in this case R_1= drop radii and $R_2 \longrightarrow \infty$).

In order to have accurate information about IFT, which is important in liquid-liquid dispersion because of its influence on drop breakage, the device was deeply cleaned and the measurement were made at a temperature of 20°C.
A sample of each solvent was taken and poured into a burette.
The 0,5 mm needle was inserted in the burette until the tip was submerged in the sample.

Than water was insufflate in the needle and droplets were created in the oil-phase.

After each solvent measurement the device was deep cleaned with UP water, pure acetone and than dryed with air.

Than the SFT values for purified water (72 mN/m) was measured , in order to verify the complete cleaning of the instrument.

The data collecting calculated the IFT values according to this set of parameters:

- density of water (994,6 kg/m^3)
- temperature density of the drop (at the same temperature of the measurement)

For each solvent a set of at least 10 were taken.

The measures for Wacker Silicones dimethicone revealed a really low difference in the density compared to water, so the size of drops were too big to be completly taken by the camera.

To afford the value for the interfacial tension of this solvent a ring tensiometer (Krüss K 8600) was used. (Gores 2003).

Refrax Index

The Refrax Index (n) is another property of great importance for this work: this research is based mostly on image-datas taken with an endoscope and the refractive index n is of great importance for the sharpness and quality of the pictures taken.

The measurements were made putting a couple of drops of solvent on the lense of the device for measurement, paying particular attention to avoid the creation of small air bubbles in it.

Than the refrax index values obtained where recorded. Each solvent measuring was repeated 3 times.

Also in this case, like for the IFT measurements, after each solvent the device was deeply cleaned (with surfactant solution and water) and than the RI for water (n_W=1,333) was verified in order to confirm the cleaning of the lense.

Viscosity

To measure the viscosity the the falling sphere viscometer was used. A rotating-viscosimeter was tested too, but gave unreasonalble results due to the low viscosity. of the chosen solvents .

The clear-glass pipe was filled with the solvent and than a glass sphere (d_{sph}= 0,0158 m) was inserted, chosen according to the viscosity range of the oils.

The pipe was turned several time to check that no air bubbles were left inside, which could compromise the race of the sphere and than the results.

With a chronometer the passing time of the glass sphere between two lines was taken for 3 times for each oil.

With this measured time value it was possible to calculate the viscosity according to the following equation:

$$\eta_{din} = F \cdot K \cdot (S_k - S_f) \quad (10)$$

where F is the fall time, K is the sphere constant (0,008 in this case) and S_k and S_f are the sphere and the liquid density respectively.

The density of the sphere (2,22351 kg/m^3) was calculated knowing its diameter (d_{sph}= 0,0158 m) and mass (m_{sph}= 0,004592kg).

After each solvent the device was deeply cleaned, filled with water and the dynamic viscosity for water (around 1cP) was verified in order to confirm the perfect cleaning of the equipments.

With Eq. (10) the dynamic viscosity values were calculated and with the density, measured at the same temperature, the kinematic viscosity was obtained.

Density

The density measurements were made with a laboratory balance.

A sample of each solvent was taken and the density was measured, knowing the volume of sample used. The measurements were made at 20°C.

4. Results and discussion

4.1. Physical properties of the different oils

The physical properties of the dispersed phase have got a great influence on the drop size distribution and on the quality of images taken with the endoscope.

As it was mentioned above, in order to find a solvent which could take the place of the toluene, its properties (Tab. 4) have been taken as a model for choosing the new dispersed phase.

Tab. 4: Toluene physical properties

Physical State	Clear liquid
ν_{kin} [mm²/s] (20°C)	0,7
n (20°C)	1,496
ρ [kg/m^3] (20°C)	866
γ [mN/m] (20°C)	35
σ [mN/m] (20°C)	26,6
Danger	Flammable

The physical properties have been measured and compared to the corresponding toluene values and the sellers' datas, as it is reported below.

Index of refraction

Because of the great importance of the sharpness of images taken with the endoscope, the index of refraction of the different oils has been tested.

The refractive index of the dispersed phase influences the optical properties of the pictures. To make the phase surface visible the refractive index of the dispersed phase should be different from that of the continuous phase water (n_w=1,333).

In Tab. 5 the values of the refrax index measurements are summarized.

Tab. 5 : Values for the refrax index

	Roth silicon oil M3	**Wacker Silicones dimethicone**	**Fauth paraffin oil FC1013**	**Fauth paraffin oil FC1013**	**Fauth paraffin oil FC2006**	**Mobil velocite oil 3 system**
ch.no.	479150037	OM24819	Sample Fauth 31.03.2010	1300038	Sample Fauth 31.03.2010	J01032003 2100049
n [-] measured values (25°C)	1,3928	1,3982	1,4196	1,4187	1,4551	1,4475
n [-] sellers' values	-	1,396 **(25°C)**	>1,4180 **(15°C)**	>1,4180 **(15°C)**	-	-
Physical state	Clear liquid	Clear liquid	Clear liquid	Clear liquid	Clear liquid	Light yellow liquid

The measured values are all in the interval given by the sellers. They are all a little smller than the toluene one (n_{tol}=1,496).

The values for Fauth paraffin oil FC2006 and Mobile velocite oil 3 are the highest and therefore closest ones to the value of toluene.

Fig.13 shows example pictures of the different oils.

As it can be seen the quality of all pictures is worst compared to the toluene ones.

The toluene and Roth silicon oil M3 images are the sharpest while the Mobile velocite oil 3 and Fauth paraffin oil FC2006 ones are the worst ones.

Other parameters influence therefore strongly the quality and sharpness of the enoscope pictures

It has also to be noticed that the Mobile velocite oil 3 was the only dispersed phase without clear-liquid aspect, as shows Tab.5. This might have played a role in the quality of images taken by the endoscope (Fig. 13).

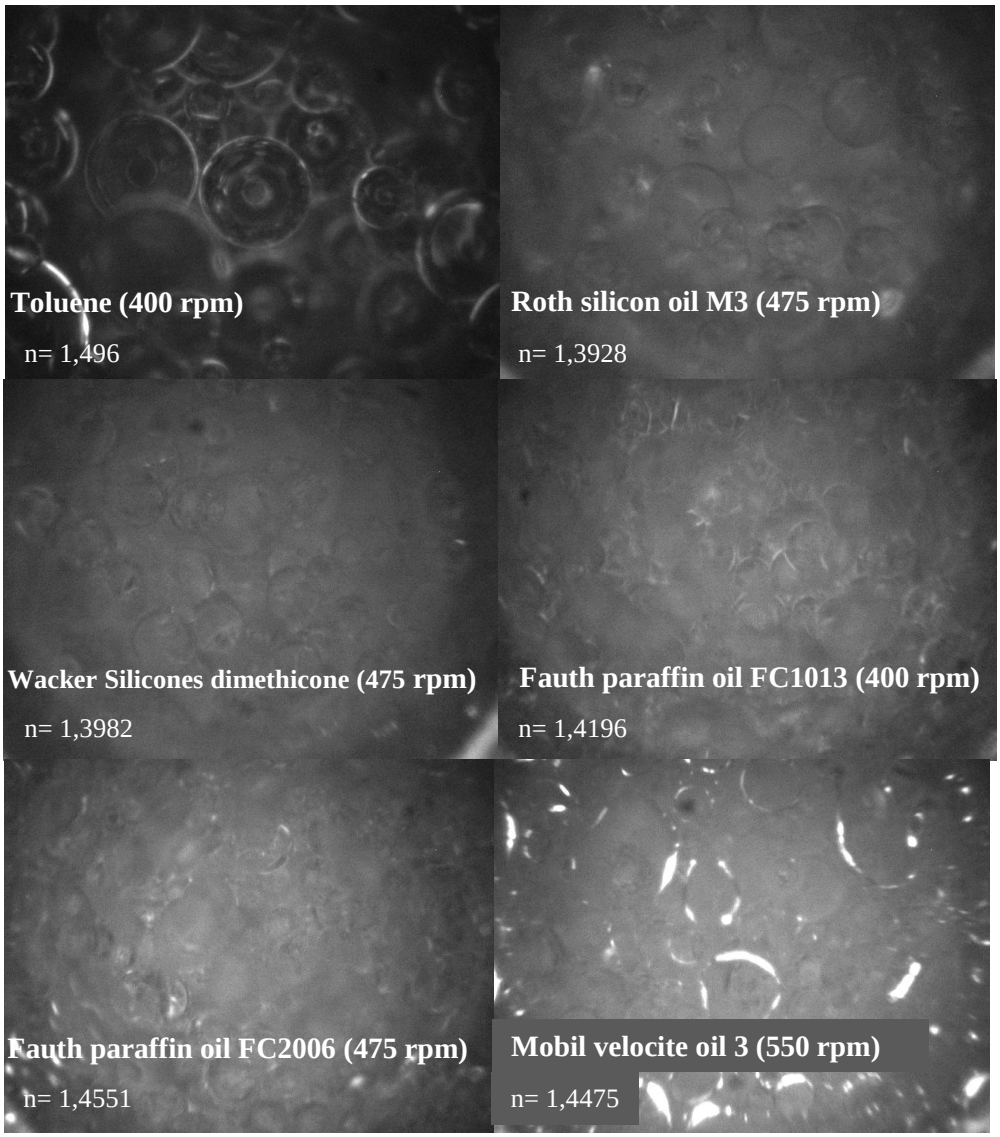

Fig. 13: Example of images taken with the endoscope for each solvent, at the lower speed experiment, after 1 minute of agitation.

Density

The values of density for the dispersed phases are summarised in Tab.6. The measured values are comparable to the sellers' ones, even if for the Roth silicon oil M3 the measured values are a bit lower.

This can be explained by the great effect of the temperature on the density values: measurement at higher temperature led to smaller values.

Due to the high temperature in the laboratory a temperature increase during the measurements could not be hindered, although the samples were stored and cooled in the fridge.

Tab. 6: Solvents densities

	Roth silicon oil M3	**Wacker Silicones dimethicone**	**Fauth paraffin oil FC1013**	**Fauth paraffin oil FC1013**	**Fauth paraffin oil FC2006**	**Mobil velocite oil 3 system**
ch.no.	479150037	OM24819	Sample Fauth 31.03.2010	1300038	Sample Fauth 31.03.2010	J010320032 100049
ρ [kg/ m^3] (20°C) measured value	881,6	909,6	744,8	741,6	816	805
ρ [kg/ m^3] sellers' values	900-910 **(25°C)**	920 **(25°C)**	740-760 **(15°C)**	740-760 **(15°C)**	750-850 **(15°C)**	802 **(15°C)**
ρ [kg/ m^3] (26°C) measured value	876,6	899,3	623	619	798,9	802,8

In comparison to the toluene density (ρ_{tol}= 866 kg/ m^3), the most similar value is given for the Roth silicon oil M3 one, while the lowest value is found for the Fauth paraffin oil FC1013.

Viscosity

One of the physical properties which has got a great influence on the DSD, as mentioned in Chapter 2.2 , is the viscosity. In Tab. 7 the measured values in comparison to the sellers' ones. are reported

Tab. 7: Solvents kinematic viscosity values

	Roth silicon oil M3	**Wacker Silicones dimethicone**	**Fauth paraffin oil FC1013**	**Fauth paraffin oil FC1013**	**Fauth paraffin oil FC2006**	**Mobil velocite oil 3 system**
ch.no.	479150037	OM24819	Sample Fauth 31.03.2010	1300038	Sample Fauth 31.03.2010	J01032003 2100049
ν_{kin} [mm²/s] (26°C) measured values	2,910	7,711	2,192	2,267	10,119	2,174
ν_{kin} [mm²/s] sellers' values	10 **(25°C)**	5 **(25°C)**	1,5-2,15 **(20°C)**	1,5-2,15 **(20°C)**	9,5-16 **(20°C)**	2 **(40°C)**

The measured values are comparable to the sellers‘ ones, except for the Roth Silicon oil M3, which has got much higher values at lightly lower temperature.

In general the kinematic viscosity values of the dispersed phase are all higer than the toluen one ($\nu_{kin,tol}$ =0,7 mm²/s), expecially for Wacker Silicones dimethicone and Fauth paraffin oil FC2006.

IFT

The interfacial tension strongly influences the drop breakage processes and was therefore measured against water

Results, averaged from 10 measurements, are shown in the Tab.8.

Tab. 8: Measured IFT values

	Roth silicon oil M3	**Wacker Silicones dimethicone**	**Fauth paraffin oil FC1013**	**Fauth paraffin oil FC1013**	**Fauth paraffin oil FC2006**	**Mobil velocite oil 3 system**
ch.no.	479150037	OM24819	Sample Fauth 31.03.2010	1300038	Sample Fauth 31.03.2010	J01032003 2100049
γ [mN/m] (20°C) measured values	39,8± 1%	34	48,5± 0,9%	49,5± 0,6%	39,2± 4,4%	16,6± 2,5%

The Wacker Silicones dimethicone and the Fauth paraffin oil FC1013 have got the closer values of the IFT to the toluene (γ_{tol}= 35 mN/m).

4.2. Investigations in the stirred tank

In a liquid/ liquid-system the analysis of the Drop Size Distribution is important in order to determine parameters involved in the mass tranfer process i.e. the interfacial area.

As mentioned in Chapter 3.2 for each dispersed phase were manually counted four series of 200 images each made with the endoscope, referred to the lowest and the highest velocity, at the first and at the last time step.

Going through each picture, using Boubble Count (BC), the sharpest droplets were choosen and their cumulative probability was calculated, as well as the Sauter diameter.

Toluene

Three experiments were carried out with toluene. Stirrer speeds of 400, 550 and 700 rpm were applied. The coalescence behaviour was not investigated for this solvent. Gäbler et al. (2006) already studied the coalescence-behaviour of toluene/water systems. At a pH-value of 7 it is very fast-coalescing and after one minute of stirring the steady-state is already reached.

The images taken in each experiment, after setting the endoscope parameters, were sharp as Fig. 14 reveals.

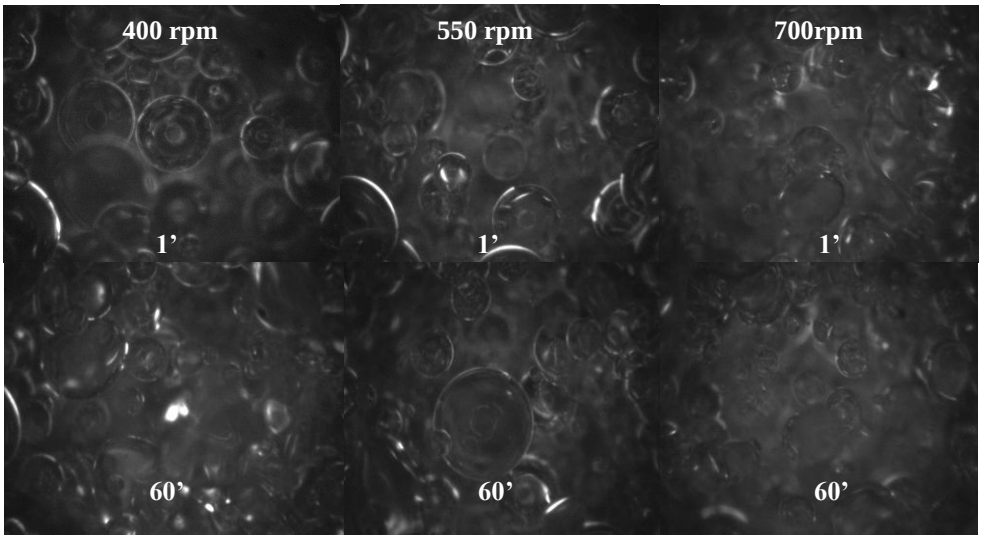

Fig. 14: Example of toluene images at different stirrer speed and time

The Boubble Count results are summarized in Fig. 15 and Tab.9.

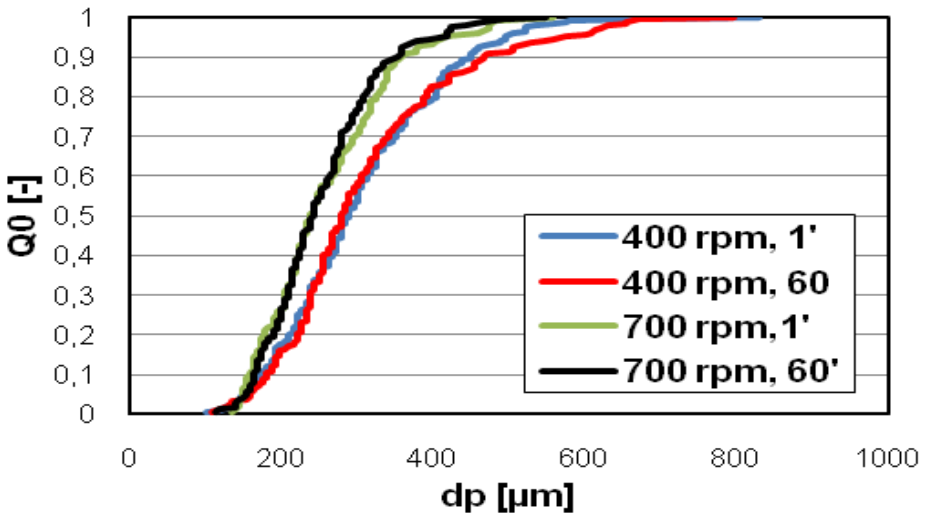

Fig. 15: Distributions of drop sizes, Sauter diameter and number of counted drops for a toluene/water system

Tab. 9: Manual counting with BC for toluene

speed [rpm]	time [min]	st dev/d32 [-]	d_32 [µm]
400	1	0,2831	384,297
400	60	0,294	413,490
700	1	0,267	315,870
700	60	0,252	301,860

As expected from the analysis of the breakage forces, which depends from the turbulent field generated and so from the stirrer speed, the Sauter diameter become smaller as experiment speed increase.

It is also noticeble that d_{32} increase with the time, instead of decreasing as expected, for the lower speed experiment.

As it is known, that steady-state is reached after one minute. Therefore the Sauter mean diameter should not differ between the two time steps.

The IPP -30 device was not working during the experiment at the higher stirrer speed (700rpm). It did not recognize droplets and no signals were transfered even if its position was changed.

However, the data collected at the lower stirrer speed were analyzed. The comparison with the manual counting value revealed that the results given from IPP-30 were unreasonable, the IPP 30 reconizes much bigger drops, which leads to a larger Sauter mean diameter (Fig. 16 and Tab. 10).

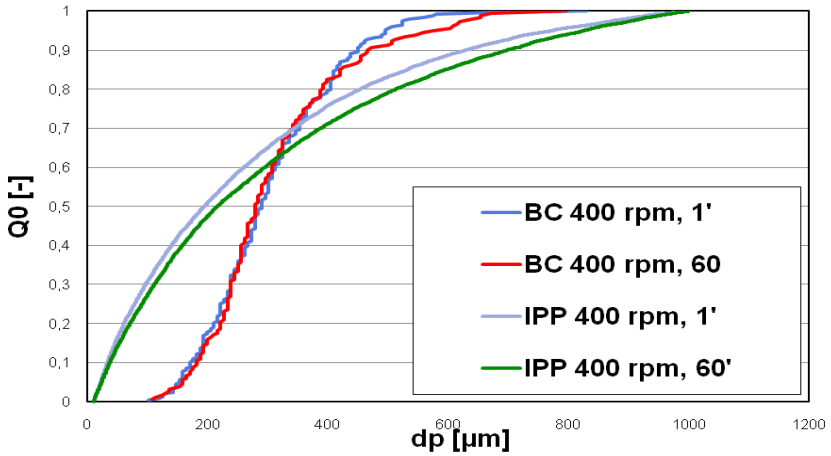

Fig. 16: Toluene BC and IPP results comparison

Tab. 10: Comparison BC-IPP for toluene

	speed [rpm]	time [min]	counted drops	d_32 [µm]
BC	400	1	248	385,3
IPP	400	1	10000	613,1
BC	700	60	182	413,4
IPP	700	60	9999	644,3

Roth Silicon oil M3

For this solvent the phase division, until a stirrer speed of 430 rpm, was noticed. The density difference between this oil and water is lower than for the the toluene-water system. This indicates that the stirrer speed of 400 rpm should be enough to disperse the oil in the continuous phase and the other physical properties mainly influence the minimum energy needed for a full dispersion. The stirrer speed was therefore set to 475.

For studying the coalescence behaviour the stirrer speed was decreased at that value after the last experiment.

Examples of images taken in each experiment with the endoscope are reported in Fig. 17.

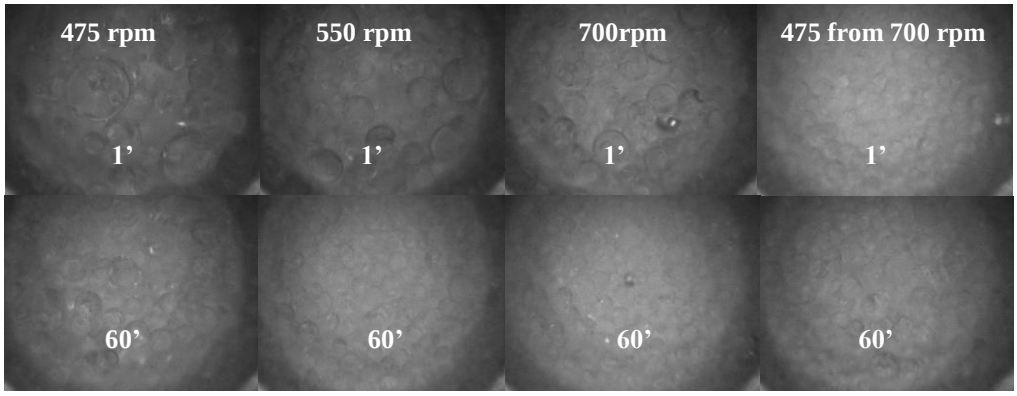

Fig. 17: Example of Roth Silicon oil M3 images at different stirrer speed and time

The quality of those images allowed the manual calculation of the drop distribution.

The Boubble Count results are summarized in Fig. 18 and Tab. 11.

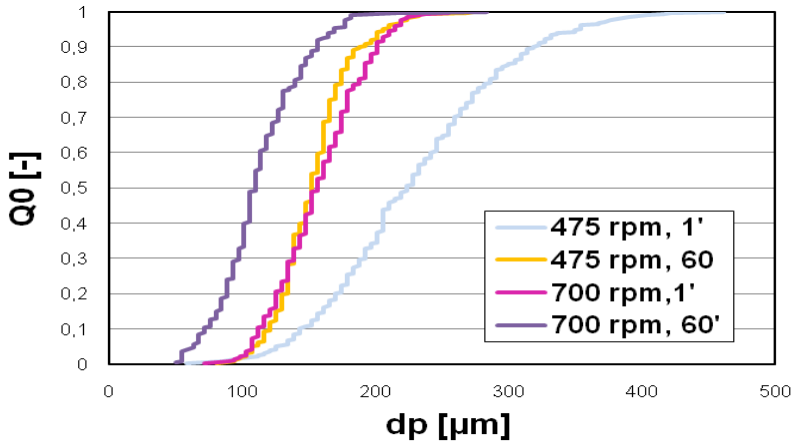

Fig. 18: Distributions of drop sizes, Sauter diameter and number of counted drops for a Roth silicon oil M3/water system

Tab. 11: Manual counting with BC for Roth silicon oil M3

speed [rpm]	time [min]	counted drops	d_32 [µm]
475	1	283	268,68
475	60	259	163,36
700	1	268	171,49
700	60	201	135,48

Also for the Roth silicon oil M3, as expected, the Sauter diameter decrease with increasing of stirrer speed and time.

The distribution and the Sauter diameters relatives to the lower speed at 60 minutes and to the higer speed at the first minute are almost the same.

The IPP -30 device was not working during this experiment.

In comparison to the toluene results, as shown in Fig. 19 and Tab. 12, the Sauter diameter is sensitivly lower for the Roth silicon oil M3 and the DSD is less wide, than in the toluene experiments.

It has to be mentioned that the lower stirrer speed for the Roth silicon oil M3 experiment was different from the toluene one.

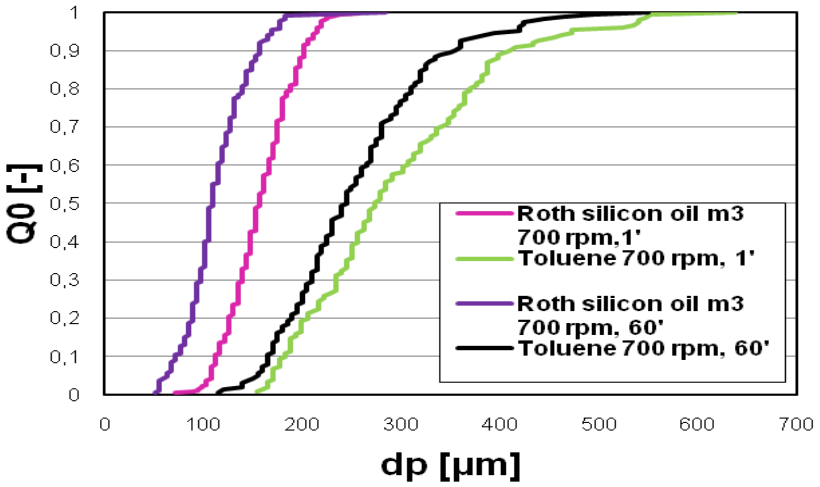

Fig. 19: Toluene and Roth silicon oil M3 comparison DSD

Tab. 12: Manual counting - comparison toluene and Roth Silicon oil M3

Dispersed phase	speed [rpm]	time [min]	d_32 [µm]
Toluene	400	1	384,29
Roth Silicon oil M3	475	1	268,68
Toluene	700	1	360,18
Roth Silicon oil M3	700	1	135,48

The Roth silicon oil M3 has got physical properties (Tab.8) in the same order than the toulene ones. The only exception is the kinematic viscosity which is higher.

The little higher interfacial tension suggests that the silicon oil droplets should be bigger than the toluene ones. One reasons for this behaviour could be that the interfacial tension is strongly changing when the system is measured in the saturated condition. The given values are for an unsaturated system. Another reason could be some impurties in the system, although everything was deeply cleaned.

Another parameter that mainly influences the drop size distribution is the coalescence behaviour. In fact, it is evident the influence of time on the DSD. Hindered coalescence leads to smaller drop sizes and a longer time until steady state is reached in comparison with non-coalescing systems.

Tab 13: Roth silicon oil M3 and Toluene physical properties comparison

	Roth silicon oil M3	**Toluene**
ν_{kyn} [mm²/s] (20°C)	2,538	0,7
n [-] measured values	1,3928	1,496
ρ [kg/m3] (20°C)	881,6	866
γ [mN/m] (20°C)	39,84	35
σ [mN/m]	18,62	26,6

Wacker Silicones dimethicone

For this solvent the phase division was noticed at 400 rpm and the first stirrer speed was set again to 475 rpm. At this speed there was totally dispersion of the aqueous and oil phase.

Examples of images taken in each experiment with the endoscope are reported in Fig. 20.

They are not really sharp and drops on lense have been noticed during the data acquisition. Therefore the experiment was interrupted after the investigations with 700 rpm.

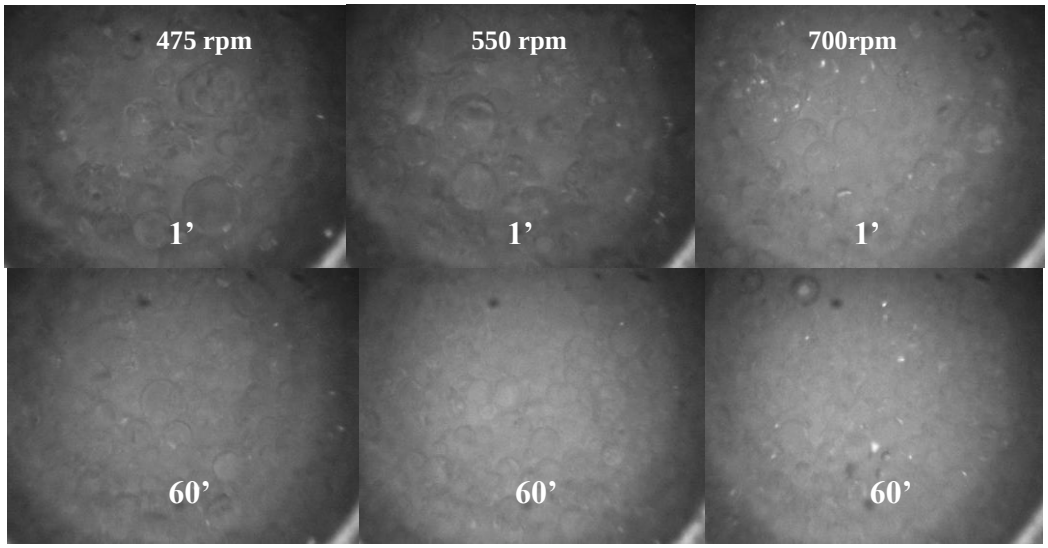

Fig. 20: Example of Wacker Silicones dimethicone images at different stirrer speed and time

The quality of those images allowed the manual calculation of the drop distribution only of the series of picture relative to the lower stirrer speed. The Bubble Count results are summarized in Fig. 21 and Tab. 14.

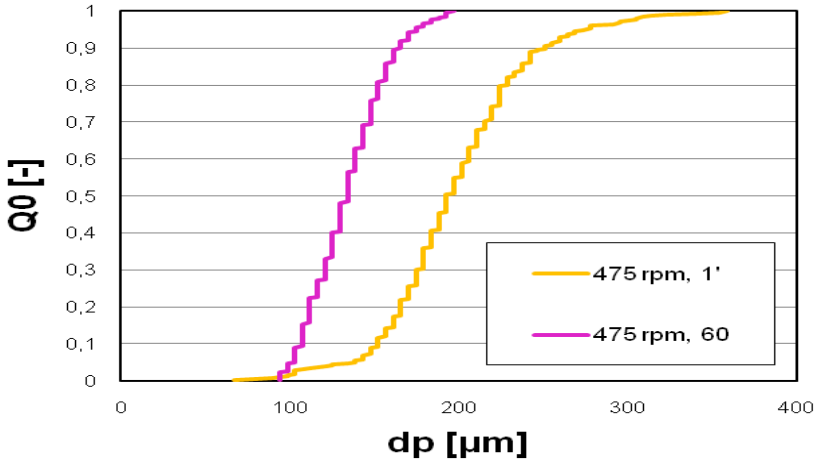

Fig. 21: Distributions of drop sizes, Sauter diameter and number of counted drops for a Wacker Silcones dimethiconee/water system

Tab 14: Manual counting with BC for for a Wacker Silcones dimethiconee/water system

speed [rpm]	time [min]	counted drops	d_32 [µm]
475	1	317	217,22
475	60	299	142,1

As expected, the Sauter diameter decrease with increasing time step.

In comparison to the toluene results, as shown in Fig. 22 and Tab.15, the Sauter diameter is sensitivly lower for the Wacker Silicones dimethicone and the DSD is less wide, than in the toluene experiments. It has to be mentioed that the stirrer speeds are different, because 400 rpm were not enough to reach complete phase dispersion of Wacker Silicones dimethicone.

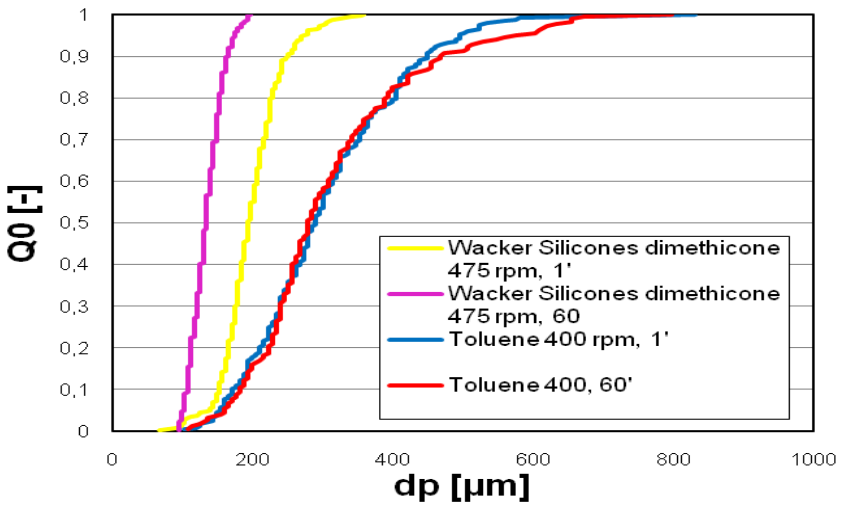

Fig. 22: Toluene and Wacker Silicones dimethiconecomparison DSD

Tab 15: Manual counting -comparison toluene and Wacker Silicones dimethicone

Dispersed phase	speed [rpm]	time [min]	d_32 [µm]
Toluene	400	1	384,29
Wacker Silicones dimethicone	475	1	217,22
Toluene	400	60	413,49
Wacker Silicones dimethicone	475	60	142,11

This can be explained by the analysis of the physical properties (Tab. 16) of Wacker Silicone dimethicone, in comparison to the toluene ones, which reveal a litter lower IFT, that highly can influence the drop size distribution .

Tab 16: Wacker Silicones dimethicone and Toluene physical properties comparison

	Wacker Silicones dimethicone	Toluene
ν_{kyn} [mm²/s] (20°C)	7,711	0,7
n [-] measured values	1,398	1,496
ρ [kg/m3] (20°C)	909,6	866
γ [mN/m] (20°C)	34	35
σ [mN/m]	16,43	26,6

Fauth paraffin oil FC1013.

For this solvent the phase division was noticed at 400 rpm and the first stirrer speed was set again at 475 rpm.

Examples of images taken in each experiment with the endoscope are reported in Fig. 23. They are not really sharp and drops on lense have been noticed. Due to this the experiment to study the coalescence behaviour was not made.

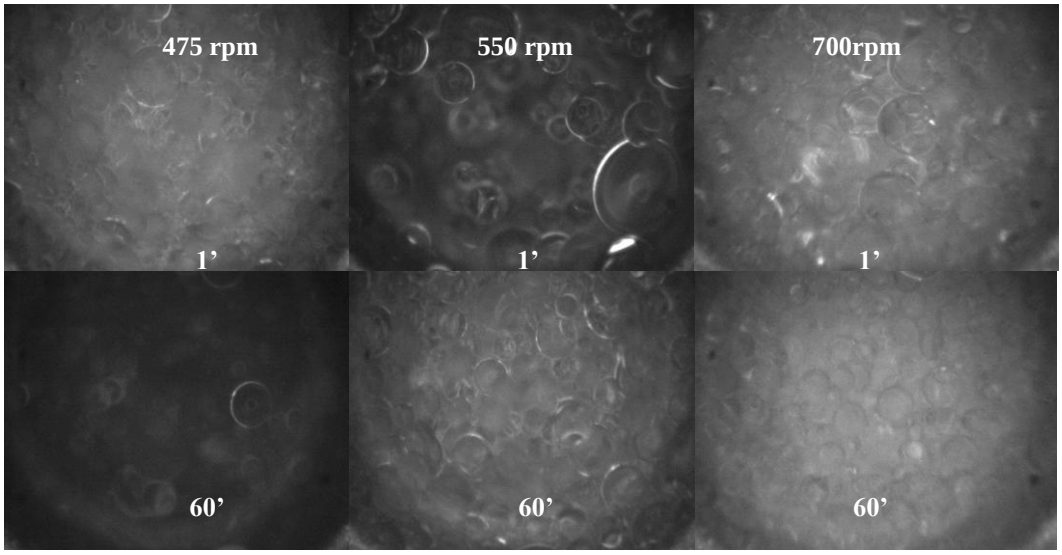

Fig. 23: Example of Fauth paraffin oil FC1013 images at different stirrer speed and time

The quality of those images allowed the manual calculation of the drop distribution. Instead of 475 rpm, the 550 rpm images were taken. The Boubble Count results are summarized in Fig.23 and Tab. 17.

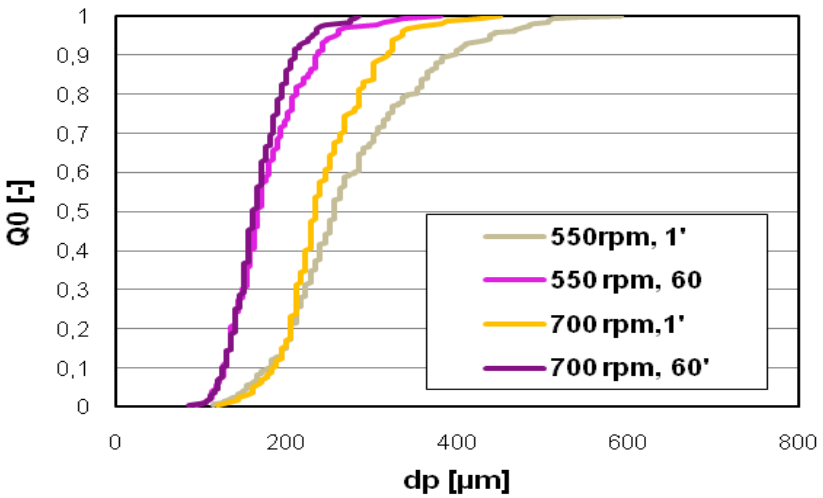

Fig.23: Distributions of drop sizes, Sauter diameter and number of counted drops for a Fauth paraffin oil FC1013/water system

Tab 17: Manual counting for Fauth paraffin oil FC1013

speed [rpm]	time [min]	counted drops	d_32 [µm]
550	1	264	329,86
550	60	175	203,06
700	1	160	268,09
700	60	188	181,51

Also for the Fauth paraffin oil FC1013, as expected, the Sauter diameter decrease with increasing of stirrer speed and time.

The particle distribution and the Sauter diameter at the higer stirrer speed after 1 minute, show higher values of d_{32} than at 500 rpm, after one hour of agitation. This results is quite unexpected but the behaviour of this dispersed phase was particular.

Infact, the quality of images taken with the endoscope, was changing according to the stirrer speed:

At the lower speed the manual counting was not possible due to the lack of sharpness, while at 550 rpm the quality of images was comparable to the toluene one. At the higer stirrer speed the sharpness decreased again but was enough for the d_{32} and DSD manual analysis

In comparison to the toluene results, as showned in Fig.24 and Tab. 18, for the Fauth paraffin oil FC1013 the DSD is shfted towards smaller particles, while the Sauter diameter is a bit lower.

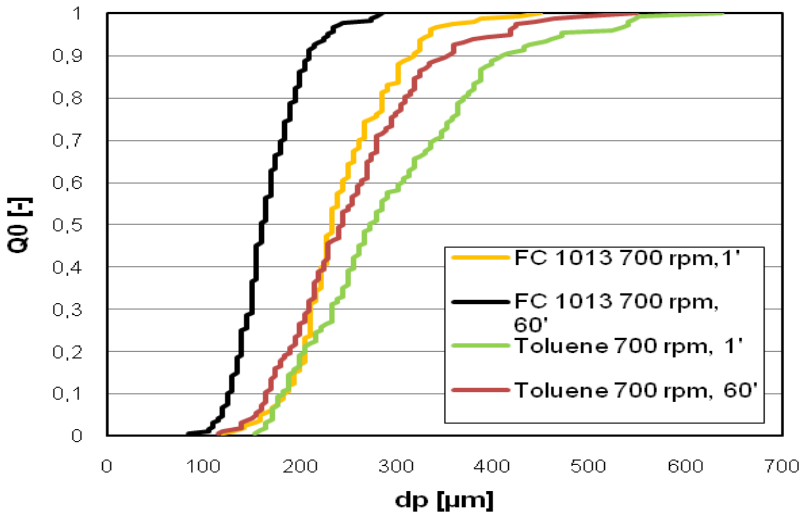

Fig. 24: Toluene and Fauth araffin oil FC1013 comparison DSD

Tab 18: Manual counting comparison- toluene and Fauth paraffin oil FC1013

Dispersed phase	speed [rpm]	time [min]	d_32 [µm]
Toluene	700	1	368,18
Fauth paraffin oil FC1013	700	1	268,09
Toluene	700	60	308,86
Fauth paraffin oil FC1013	700	60	181,55

Because the sharpness of images for this solvent was similar to the toluene pictures, Fauth paraffin oil FC1013 was, in a first moment, choosen as a good alternative.

As further experiments were planned with this solvent another charge was tested on the physical properties.The analysis, revealed a small difference in the physical properties in comparison to the first sample of the same oil (Tab.19).

Tab 19: Toluene and Fauth paraffin oil FC1013 from two different charge number, properties comparison

	Fauth paraffin oil FC1013	Fauth paraffin oil FC1013	Toluene
ch.no.	Sample Fauth 31.03.2010	1300038	-
ν_{kyn} [mm²/s] (20°C)	2,192	2,267	0,7
n [-] measured values	1,420	1,419	1,496
ρ [kg/m3] (20°C)	744,8	741,6	866
γ [mN/m] (20°C)	48,56	49,55	35

Fauth paraffin oil FC2006

The next solvent analyzed is the Fauth paraffin oil FC2006.

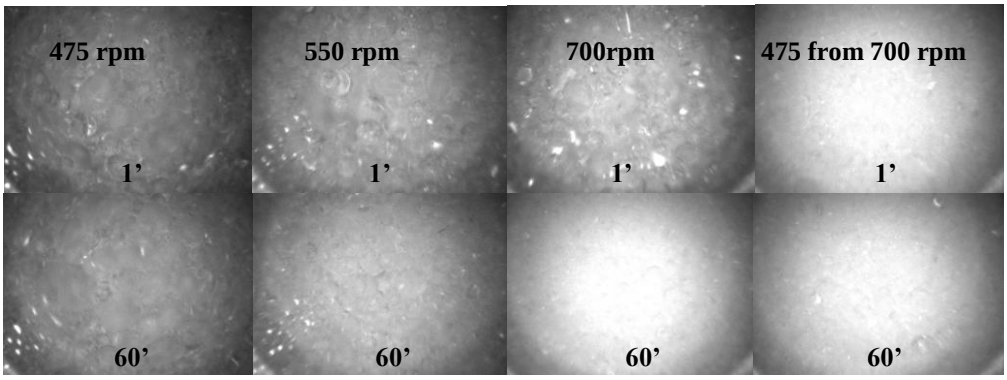

Fig. 25: Example of Fauth paraffin oil FC2006 images at different stirrer speed and time

The sharpness of images taken (Fig. 25) with the endoscope was not good enough to let analyze the DSD and the Sauter diameter, even if the physical properties (Tab. 20) encouraged good results.

The IPP-30 was not working at any stirrer speed.

Tab 20: Toluene and Fauth paraffin oil FC2006 properties comparison

	Fauth paraffin oil FC2006	**Toluene**
ν_{kyn} [mm²/s] (20°C)	10,119	0,7
n [-] measured values	1,455	1,496
ρ [kg/m3] (20°C)	816	866
γ [mN/m] (20°C)	39,27	35

Mobil velocite oil 3

This solvent presented phase division untill 500 rpm. The experiment at lower stirrer speed was made at 550 rpm.

As well as for the Fauth paraffin oil FC2006 the Mobil velocite oil 3 gave unusable images (Fig. 26), even worst than the one relative at the above mentioned solvent, even if mostly of the physical parameters are similar to the Toluene ones.

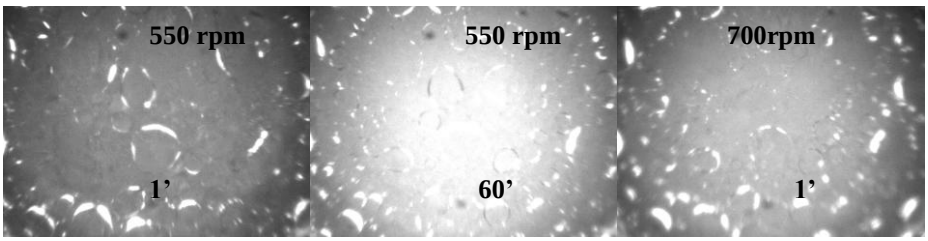

Fig. 26: Example of Fauth paraffin oil FC2006 images at different stirrer speed and time

The above images show the sharpness of pictures for the Mobil velocite oil, which was not enough for the analysis of the system with BC. Additionally drops on the endoscope lense were noticed.

Because of this reason, and because the IPP was not working, the experiment has been stopped after 20' of agitation at 700 rpm.

One reasnon that could have influenced the images sharpness is the physical aspect of this solvent.Even if the refrax index of the Mobil velocite oil 3 is quite similar to the toluene one (Tab.21), as well as other physical properties, has to be

mentioned that the aspect of this dispersed phase was a light-yellow liquid, instead of clear-liquid aspect like all the other dispersed phase. This can have had an influence on the images taken with the endoscope.

Tab 21.: Mobile velocite oil 3 and Toluene properties comparison

	Mobil velocite oil 3 system	**Toluene**
ν_{kyn} [mm²/s] (20°C)	2,080	0,7
n [-] measured values	1,448	1,496
ρ [kg/m3] (20°C)	805	866
γ [mN/m] (20°C)	16,65	35

Another aspect that has to be highlighted is that one of the main reason for which the images are not sharp is the presence of impurities.

This is much more valid for the Mobll velocite oil 3 than for the other dispersed phase: first of all because this oil is a lubrificant used in auto-sector and the purity of it is far away from the labor-purity. Additionally it is sold in a big tank from which the amount for the experiment was taken by a glass-pipette which could lead to impurities in the system.

Roth silicon oil M3 experiment with mirror

After the previous analysis of the different dispersed phases, the Roth silicon oil M3 was choosen as the best substitute for toluene.

In fact, only for that dispersed phase the images were sharp enough to allow an automatical counting with Drop Dead. In order to get better images, the experiment with Roth silicon oil M3 was repeated in the same conditions with the only difference of the addition of a mirror in front of the endoscope device in order to obtaine sharper images and increase the contrast (see Annex, Fig. A2)
This solution gave good quality images, as showned in Fig. 27.

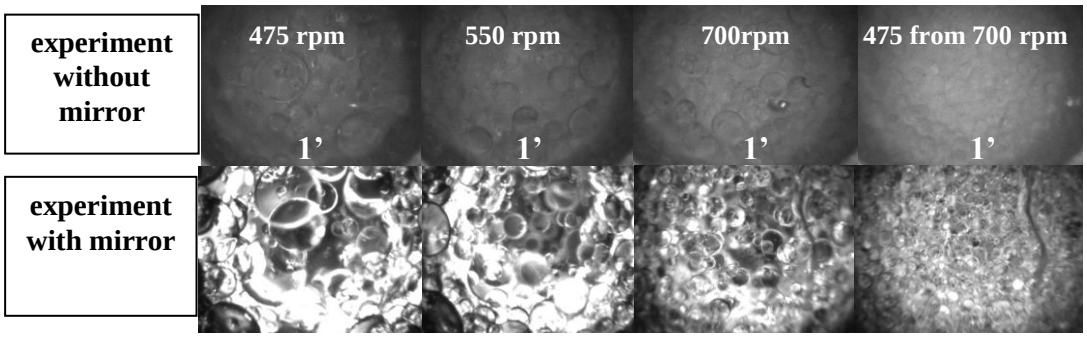

Fig.27.: Roth silicon oil M3 example of images taken in each experiment

The manual count for Roth silicon oil M3 was repeated and the results are summairzed in the Fig.28.

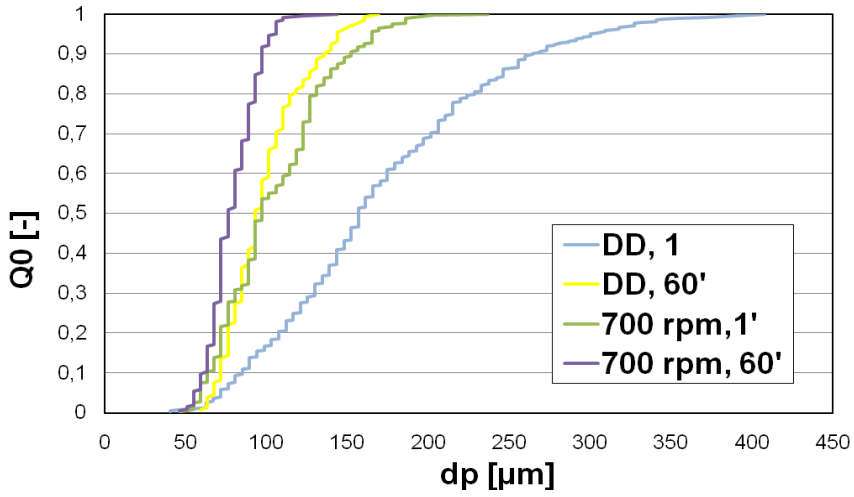

Fig 28.: Roth silicon oil M3 DSD, experiment with mirror

Tab 22.: Manual counting for Roth silicon oil M3, experiment with mirror

speed [rpm]	time [min]	counted drops	d_32 [µm]
475	1	345	254,04
475	60	213	133,11
700	1	360	126,69
700	60	204	84,91

In comparison to the experiment with the same dispersed phase (Fig. 18) and without mirror in front of the endoscope, the Sauter diameter for each experiment results a bit smaller.

DD analysis

After the manual counting for each solvent, the dispersed phases with the best images were choosen for the automatic counting with DD.
Images from toluene and Roth silicon oil M3 were choosen.

Toluol

Choosing the serie of images referred to 400 rpm and 1', DD was calibrated for toluol.

After creating a form, the influence of the border parameter classification was investigated. Four different parameter sets (DD1-DD4) were therefore tested. The calibration was repeated four times.

The diagram below (Fig. 29) shows the results obtained and highlights the high influence on the results of the border parameters calibration.

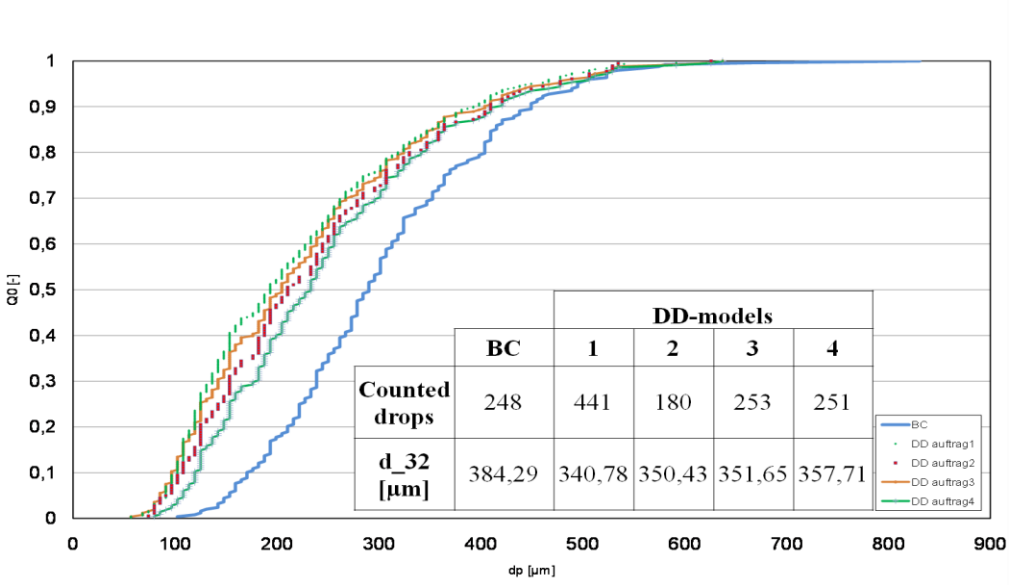

Fig 29.: Toluene DD results in comparison to the manual counting (BC)

Drop Dead determined smaller droplets for all the four parameter sets. The automatically determined sauter mean diameter, which is the closest one to the manually detected DSD is DD4, although the distribution in general is shifted towards smaller drops.

Here below is reported the comparison between the manual counting and the DD results with auftrag 4, referred to 400 rpm (Fig. 30) and 700 rpm (Fig.31).

Table are showing results of the DD calculation referred to each time step manually calculated. The DD curve are referred to the calibration serie of images.

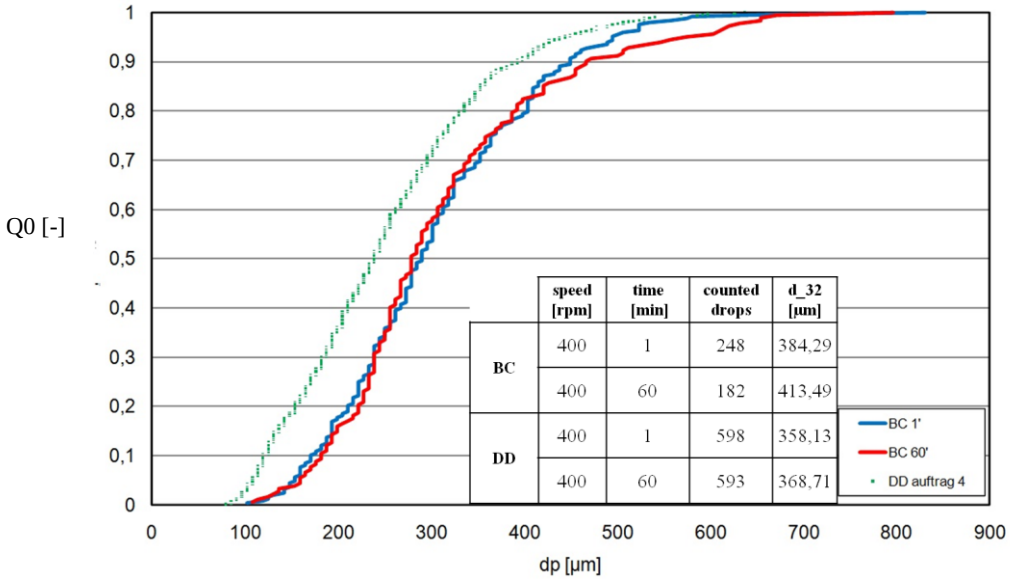

	speed [rpm]	time [min]	counted drops	d_32 [µm]
BC	400	1	248	384,29
	400	60	182	413,49
DD	400	1	598	358,13
	400	60	593	368,71

Fig 30: Toluene DD results in comparison to the manual counting (BC) at 400 rpm

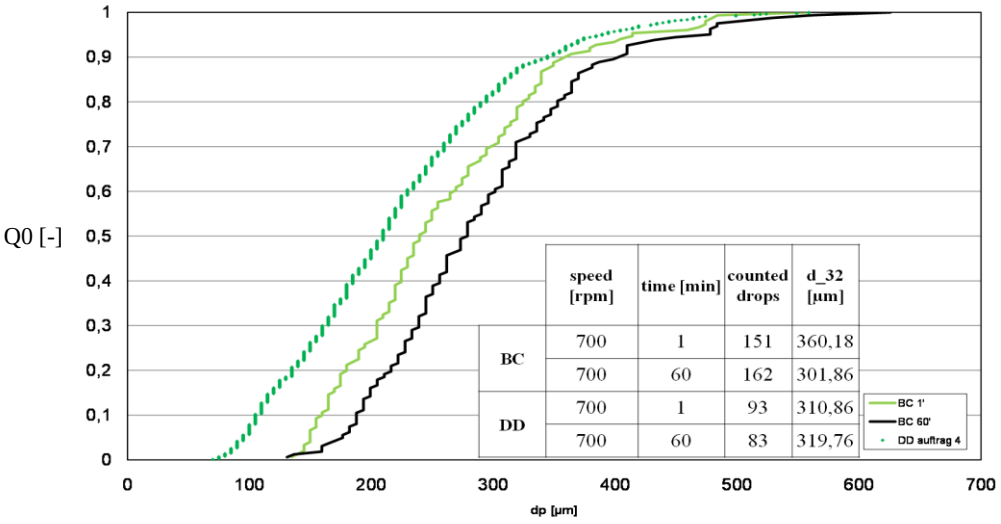

	speed [rpm]	time [min]	counted drops	d_32 [µm]
BC	700	1	151	360,18
	700	60	162	301,86
DD	700	1	93	310,86
	700	60	83	319,76

Fig 31: Toluene DD results in comparison to the manual counting (BC) at 700 rpm

Roth silicon oil M3

Similar work has been done for Roth silicon oil M3, using the images taken in the experiment wit the mirror in front of the endoscope.

Choosing the serie of images referred to the biggest drops, 475 rpm and 1', DD was calibrated for Roth silicon oil M3.

Again four different parameter sets for the border classification was tested.

The diagram annd the table below (Fig. 32, Tab. 23) shows the results obtained with the four calibration done.

The results in the table and the DSD obtained with the four DD models, highlight again the high influence on the results of the parameters calibration.

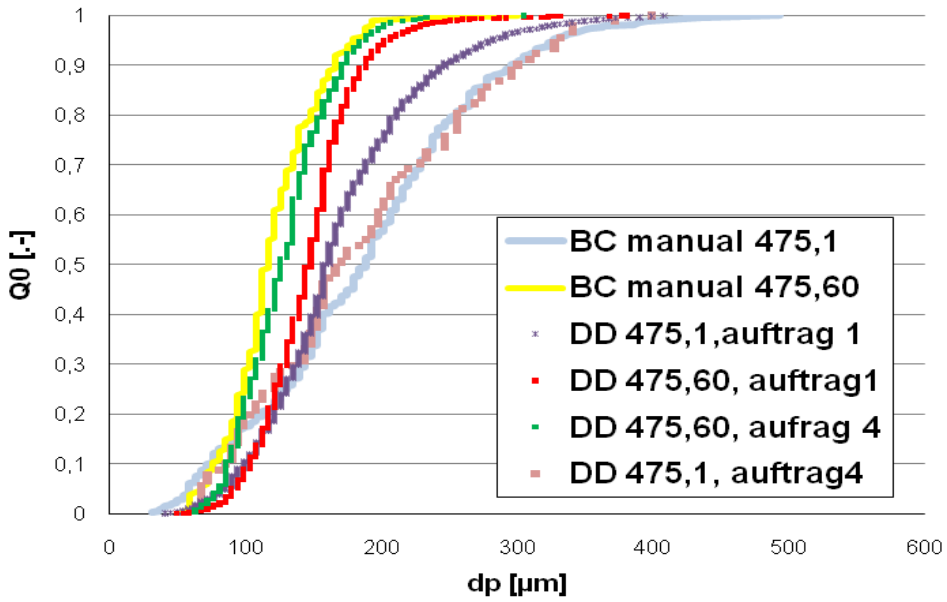

Fig. 32: Roth silicon oil M3 DD results in comparison to the manual counting (BC)

		DD- Auftrags			
	BC	**1**	**2**	**3**	**4**
Counted drops	248	441	180	253	215
d_32 [µm]	384,29	340,78	350,43	351,65	357,71

Tab 23.: Roth silicon oil M3 DD results in comparison to the manual counting (BC)

The DSD closer to the one manually calculated is the one referred to the fourth auftrag, as the Sauter diameter value confirm.

Here below is reported the comparison between the manual counting and the DD results with auftrag 4, referred to two different time steps, 475 rpm (Fig. 33).

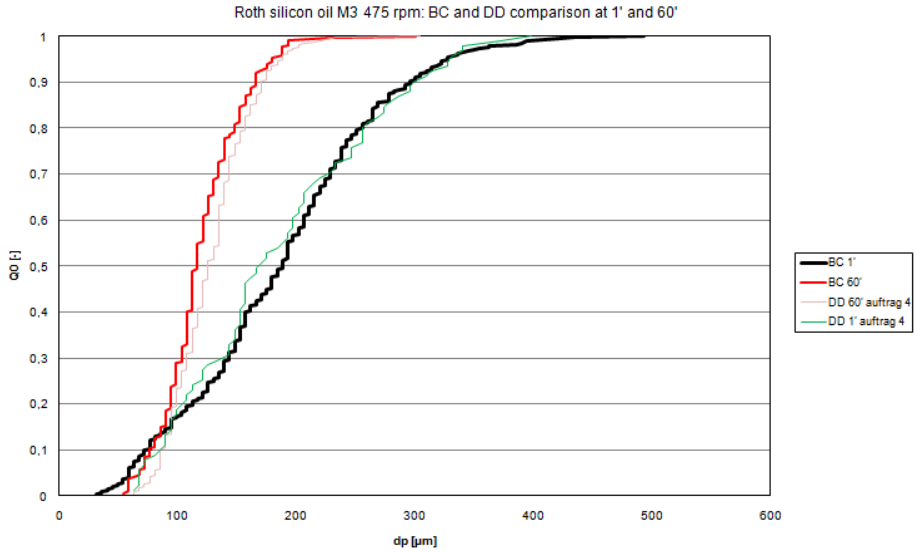

Fig.33: Roth silicon oil M3 DD and BC results at two time steps with auftrag 4

In order to show the influence of the DD parameters optimazation, the same comparison with the BC results has been done with auftrag 1, which was taking more and smaller drops.

Fig. 34 show that even if the Sauter diameter for auftrag 1 was, in first instance, not so different from the manual result, the distribution at different time steps can be really different.

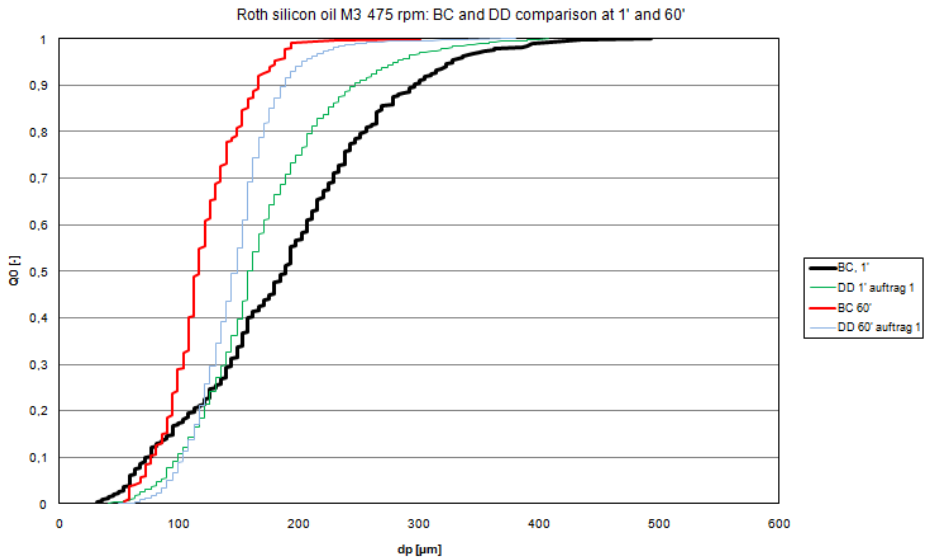

Fig.34: Roth silicon oil M3 DD and BC results at two time steps wit auftrag 1

After this proof the auftrag 4 was used for the automatical calculation with DD (See annex, Tab. A3 , Fig A5, A6, A7, A8). The diagram below (Fig. 35) shows the Sauter diameter behaviour and the drop distribution calculated at each stirrer speed, at different time steps.

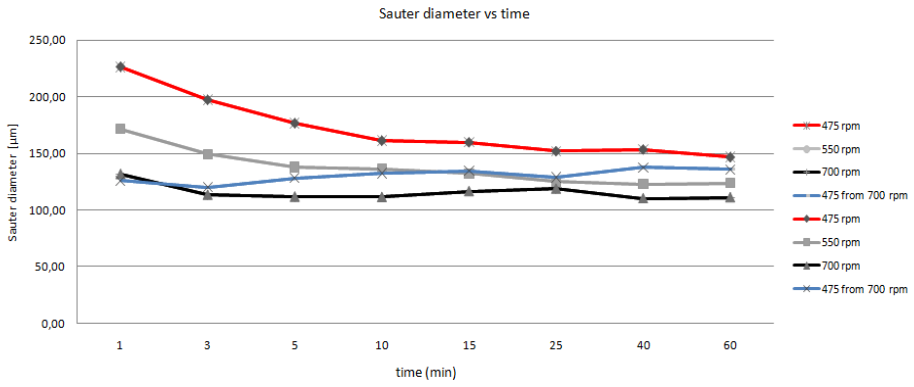

Fig. 35: Roth silicone oil M3 sauter diameter in the time, calculated with DD

The comparison of DSD with the Bubble Count is made in the following Fig. 36.

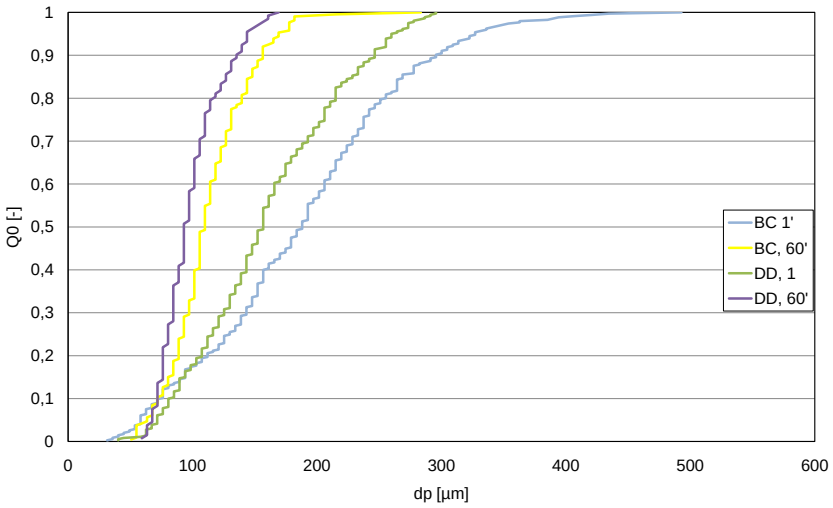

Fig. 36. Roth silicone oil M3 comparisono between DD and BC at 475 rpm

Tab.24: Roth silicon oil M3 DD results in comparison with the manual counting

		BC	DD	BC	DD
speed [rpm]	**time [min]**	**counted drops**		**d_32 [µm]**	
475	1	345	382	254,04	226,53
475	60	213	340	133,11	146,82
700	1	360	468	126,69	131,71
700	60	204	132	84,91	111,17

It's evident, also accoring to Tab.13 that DD counted smaller drops, as it was already noticed for the toluene.

Because of it the parameters setting have always to be done on the serie of images referred to the bigger drops.

5. Conclusions

The analysis of the results referred to different dispersed phases leads to the conclusion that the measurement and consideration of the physical properties are not enough to choose a dispersed phase which can be used instead of toluene.

In fact, even if the refractive index of Roth Silicon oil M3 was one of the most different from the toluene, the resulting images given by the endoscope were the sharpest ones.

According to the analysis of quality of images, the dispersed phase that might be a good substitute for the toluene is therefore the Roth silicon oil M3.

With this solvent it was possible to use the automatic program Drop Dead and analyze the DSD and the Sauter diameter at different time steps and stirrer speeds.

Giving a look to the prices of the oils makes evident that this silicon oil is too expensive, in comparison to the other ones.

Another cheaper solvent that could give as good results is the Fauth paraffin oil FC1013.

In fact, images for this solvent were very sharp for a stirrer speed of 550 rpm.

The examination of the physical properties of two different charges showed that there are little differences due to different compositions.

In order to avoid these differences, always the same charge should be used to examine the drop size distribution.

The high influence of the IFT on the drop distribution bring to the conclusion that a more detailed analysis of this property should be done.

Only the interfacial tension in systems, which were not saturated against each other, was measured until now.

All the droplets of the oils were smaller as they were expected, due to measured interfacial tensions.

Therefore the interfacial tension should be measured again in the systems, after saturating the two phases against each other.

Another parameter that mainly influences the drop size distribution is the coalescence behaviour. In fact, it is evident the influence of the time on the DSD.

Hindered coalescennce leads to smaller drop sizes and longer time until steady state is reached in comparison with non-coalescing systems.

The endoscope device, with a mirror in front of the lense was giving more contrast to the image and should also be tested for the Fauth paraffin oil FC 1013. The IPP-30 was only suitable for toluene and Fauth paraffin oil FC 1013.

For all the other dispersed phases no droplets could be recognized, but the results given were unreasonable.

6. Bibliography

E.Y. Arashiro and N. R. Demarquette (1999). "Use of the Pendant Drop Method to Measure Interfacial Tension between Molten Polymers." Materials Research **2**(1): 23-32.

R.V. Calabrese, T.P.K. Chang and P.T. Dang (1986). "Drop Breakup in Turbulent Stirred-Tank Contactors". *AiChE Journal* **32**(4): 657-662.

Chesters A. K.(1991): "The modelling of coalescence processes in fluid-liquid dispersions: A review of current understanding"; *Trans IchemE*., **69:** 295-270.

EL-Hamouz, A. (2009). "Drop size distribution in a standard twin-impeller batch mixer at high dispersed-phase volume fraction". *Chem. Enf. Technol***.32** (8) : 1203-1210.

El-Hamouz, M. Cooke, A. Kawalski, P. Sharrat., (2009). Dispersion of silicone oil in water surfactant solution: Effect of impeller speed, oil viscosity and addition point on drop size distribution. *Chem. Eng. Proc* **48**, 633

Gäbler, M. Wegener, A.R. Paschedag, M. Kraume (2006). "The effect of pH on experimental and simulation results of transient drop size distributions in stirred liquid-liquid dispersion". *Chem. Eng. Sci.* **61**(9): 3018-3024.

Gores, H.-J., 2003-2004, Grenzflächenspannung, Anleitung PC-II Praktikum

R.Espejo Guardiola (2008) "Influence of the dispersed phase fraction on drop sizes in liquid/liquid systems" *Diplomarbeit.*

J.O. Hinze (1955), "Fundamentals of the hydrodynamic mechanism of splitting in dispersion process". *AiChE\ Journal* **3**(1): 289-295

Hu, B., Angeli, P., Matar, O.K., Lawrence, C.J. and Hewitt, G.F., (2006). Evaluation of drop size distributions of stirred liquid-liquid dispersions. *Chem. Eng. Technol*., **27**(3)330-334.

A.N. Kolmogoroff.(1941): "The local structure of turbulence in incompressible viscous fluid for very high Reynolds numbers", *Dokl. Akad. Nauk SSSR*, **30**: 299-303.

Kraume M. (2003): "Mischen und Rühren" Wiley-VCH Verlag Weinheim

M. Kraume, A. Gäbler, K. Schulze (2004). "Influence of physical properties on drop size distributions of stirred liquid-liquid dispersions." Chem. Eng. & Tech. **27**(3): 330-334.

E. Lutz (2008) "Analyse ein- und mehrstufiger Balkenrührwerke für die PVC-Produktion" *Diplomarbeit.*

S. Maaß, A. Gäbler, M. Wegener, A. Zaccone, A. Paschedag, M.Kraume (2007). "Drop breakage and daughter drop distributions in stirred liquid/liquid systems and their modelling within the population balance equation. *Chem. Eng. Res. Des.* **85**, 703 (2007)

S. Maaß, S.Wollny, A. Voigt , M.Kraume (2009). "Overview and experimental comparison of measurement techniques for drop size distributions in liquid/liquid dispersions". *Experiments in Fluids , accepted DOI 10.1007/s00348-010-0918-9*

S. Maaß, J. Rojahn, R. Hänsch, M. Kraume (2010). "Automated image processing for in-situ observation and control of multiphase dispersions occurring in chemical and process engineering".

P.K. Mondal, R. Sarkar, B. K. Chatterjee (2010): "A new method for measurement of droplet size distribution in superheated emulsions", *Meas. Sci. Technol*, **21** :045104 (6pp).

Pacek, A.W., I.P.T., Nienow, A.W. and Calabrese, R.V., (1994). Video Technique for Measuring Dynamics of Liquid-Liquid Dispersion during Phase Inversion. *AIChe J.*, **40**(12):1940-1949.

Parsum (2007) "Operating Manual In-line Particle Probe IPP 70".

D. Petrak (2002) "Simultaneous Measurement of Particle Size and Particle Velocity by the spatial Filtering Thechnique" *Part. Syst. Charact.* **19** : 391-400.

P. Schuchmann and T. Danner (2004): "Emulgieren: Mehr als nur Zerkleiner"; *Chemie Ingenieur Technik* **76**(4): 364-375.

R. Shinnar, J.M.Church (1960). "Predicting particle size in agitated dispersions". *Industrial and engineering chemistry* **52** (3):253-256.

R. Shinnar (1961), " On the behaviour of liquid dispersions in mixing vessels", *Journal of Fluid Mechanics* **10** (2): 259-275

C.Weng, N.T. Nguyen, T.N. Wong (2006): "Optical measurement of flow field and concentration field inside a moving nanoliter droplet", *Sensors and Actuators* **A 133** (317-322).

7. Annex

Tab.A1 . : Endoscope set up parameters

Dispersed phase	Phasenanteil [0-1]	V Disp. [ml]	V Wasser [ml]	n [rpm]	Exposure time [ms]	Brightness	Gain	Focus
Toluene	0,1	258	2322	400	25	183	645	1,5
Toluene	0,1	258	2322	550	25	183	597	1,5
Toluene	0,1	258	2322	700	25	183	589	2
Paraffinöl FC1013 [Fauth 30.03.2010]	0,1	258	2322	400	25	157	680	1,5
Paraffinöl FC1013 [Fauth 30.03.2010]	0,1	258	2322	550	25	157	680	1,5
Paraffinöl FC1013 [Fauth 30.03.2010]	0,1	258	2322	700	23	200	680	2
Paraffinöl FC2006 [Fauth 30.03.2010]	0,1	258	2322	475 after 700	27	58	680	2
Paraffinöl FC2006 [Fauth 30.03.2010]	0,1	258	2322	475	27	166	680	1,5
Paraffinöl FC2006 [Fauth 30.03.2010]	0,1	258	2322	550	23	150	680	2,5
Paraffinöl FC2006 [Fauth 30.03.2010]	0,1	258	2322	700	35	58	680	2,5
Siliconöl M3 [Ch.no. 479150037]	0,1	258	2322	475 after700	26	255	680	2,5
Siliconöl M3 [Ch.no. 479150037]	0,1	258	2322	475	25	255	680	2,5
Siliconöl M3 [Ch.no. 479150037]	0,1	258	2322	550	13	255	680	2,5
Siliconöl M3 [Ch.no. 479150037]	0,1	258	2322	700	20	197	680	2,5
Dimethicone [OM 24819]	0,1	258	2322	475 after 700	29	200	680	2,5
Dimethicone [OM 24819]	0,1	258	2322	475	29	198	680	2,5
Dimethicone [OM 24819]	0,1	258	2322	550	27	200	680	2,5
Dimethicone [OM 24819]	0,1	258	2322	700	36	200	680	2,5
Mobil Velocite no.3 (J010320032100049)	0,1	258	2322	550	31	255	680	2,5
Mobil Velocite no.3 (J010320032100049)	0,1	258	2322	700	31	50	621	3
Siliconöl M3 [Ch.no. 479150037]	0,1	258	2322	475 after700	0	0	0	2,5
Siliconöl M3 [Ch.no. 479150037]	0,1	258	2322	475	0	0	0	2,5
Siliconöl M3 [Ch.no. 479150037]	0,1	258	2322	550	0	0	0	3
Siliconöl M3 [Ch.no. 479150037]	0,1	258	2322	700	0	0	0	3

Tab A2.: Toluene Sauter diameters and counted drops with DD

400 rpm			550 rpm			700 rpm		
time (min)	**counted drops**	**d_32 [µm]**	**time (min)**	**counted drops**	**d_32 [µm]**	**time (min)**	**counted drops**	**d_32 [µm]**
1	598	358,13	1	298	364,87	1	93	310,86
3	544	365,52	3	320	350,05	3	90	307,44
5	534	354,55	5	298	352,67	5	99	311,59
10	574	356,78	10	290	249,63	10	94	319,77
15	585	365,67	15	285	347,31	15	95	321,5
25	584	358,65	25	296	349,96	25	99	315,7
40	582	357,31	40	284	359,25	40	87	299,28
60	593	368,71	60			60	83	319,76

Tab. A3: Roth silicone oil M3 Sauter diameter in the time, calculated with DD

475 rpm			550 rpm			700 rpm			475 from 700 rpm		
time (min)	**counted drops**	**d_32 [µm]**	**time (min)**	**counted drops**	**d_32 [µm]**	**time (min)**	**counted drops**	**d_32 [µm]**	**time (min)**	**counted drops**	**d_32 [µm]**
1	382	226,53	1	313	171,70	1	468	131,71	1	155	125,78
3	391	197,37	3	343	149,49	3	251	113,39	3	183	120,19
5	398	176,81	5	469	137,99	5	261	111,65	5	236	128,27
10	376	161,39	10	421	136,56	10	260	111,42	10	219	132,49
15	361	159,93	15	414	132,35	15	200	116,57	15	256	134,78
25	357	152,15	25	427	125,05	25	179	118,76	25	241	128,86
40	346	153,60	40	425	122,93	40	150	110,33	40	241	137,52
60	340	146,82	60	383	123,67	60	132	111,17	60	269	135,83

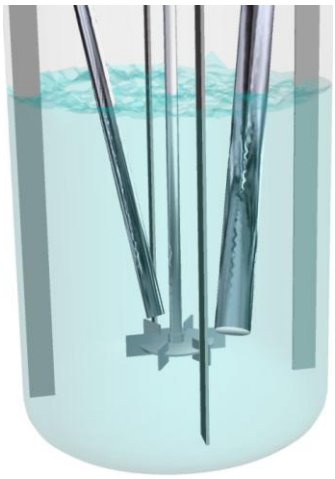

Fig. A1: Endoscope and IPP-30 position

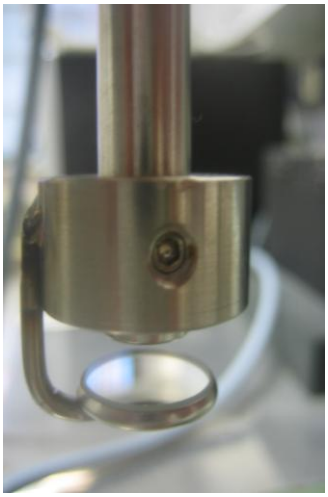

Fig. A2: Mirror device in front of the endoscope, used for second experiment with the the Roth Silicon oil M3

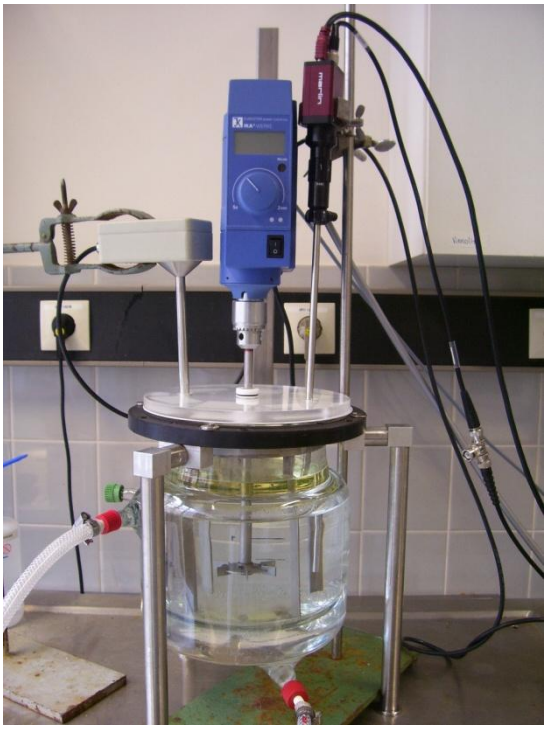

Fig. A3: Experimental setting

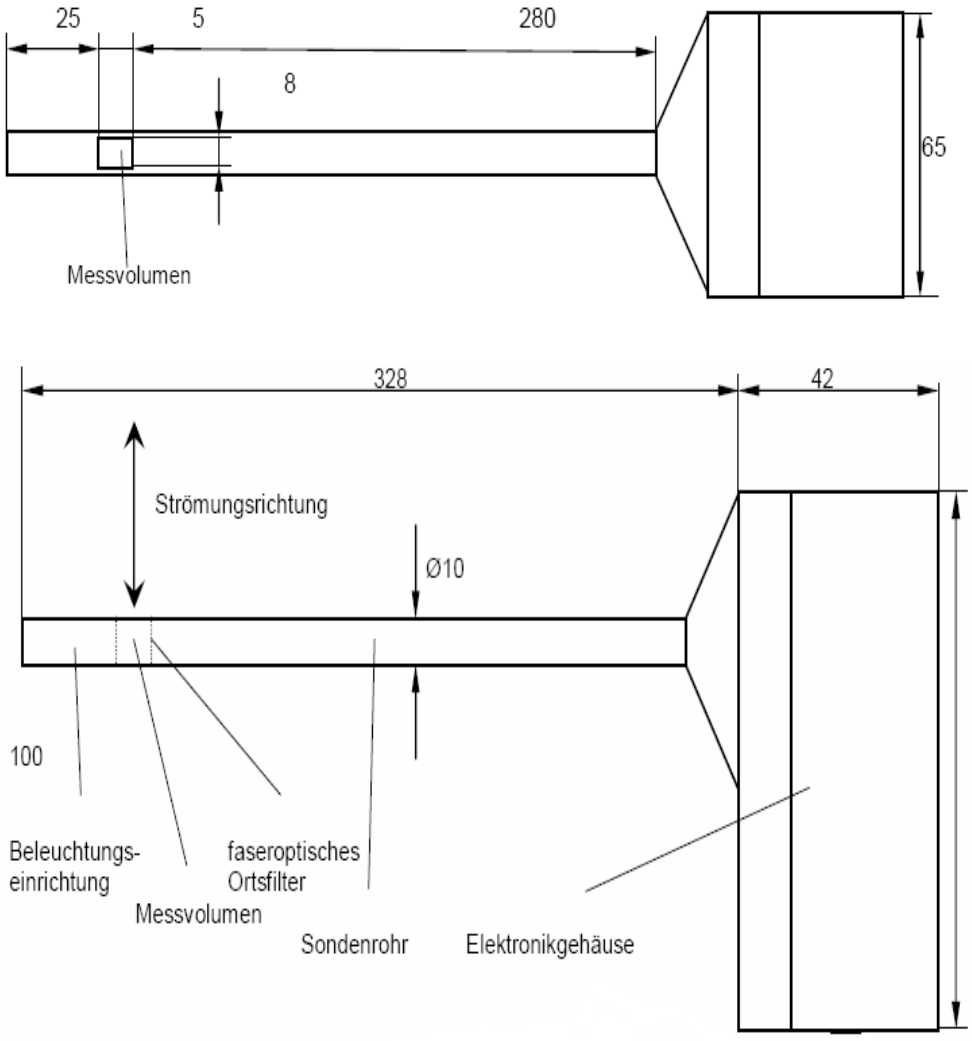

Fig A.4: IPP-30 device

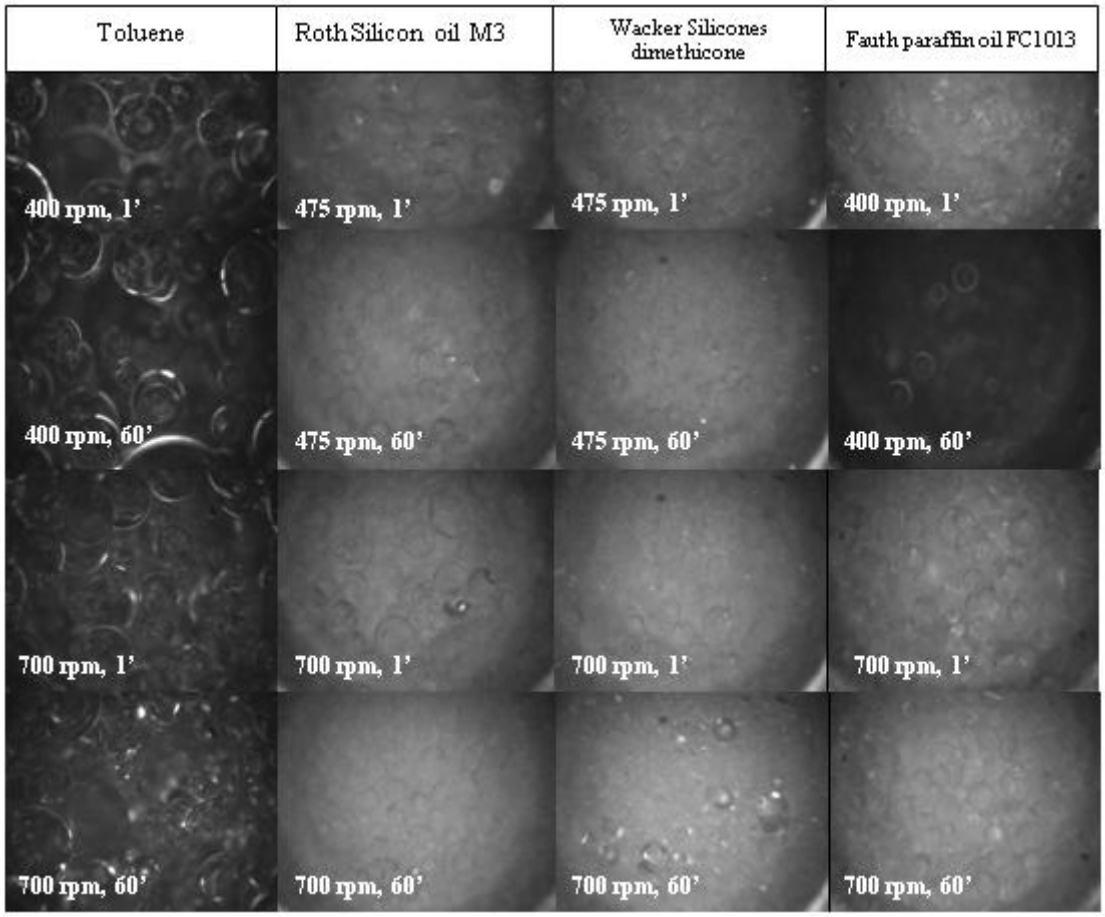

Fig. A5: Examples of images taken at different time steps and stirrer speed

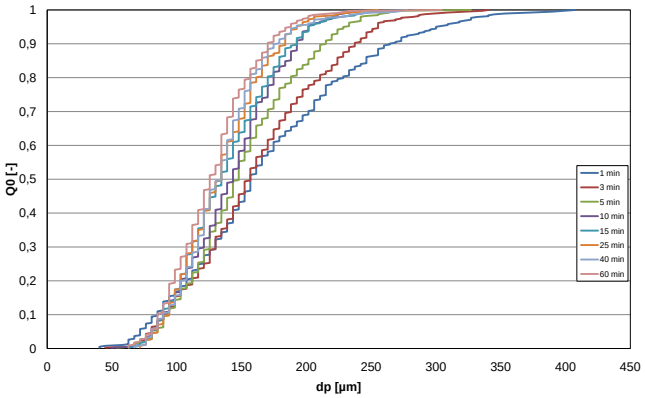

Fig. A6: Roth silicone oil M3 results at 475 rpm

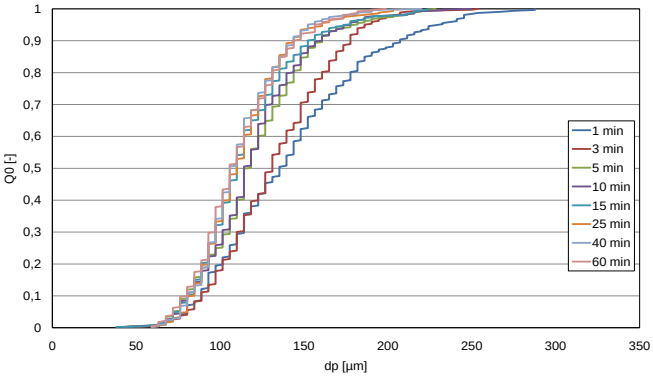

Fig. A7: Roth silicone oil M3 results at 550 rpm

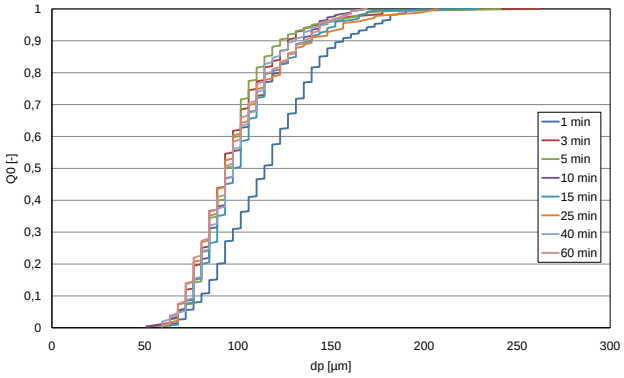

Fig. A8: Roth silicone oil M3 results at 700 rpm

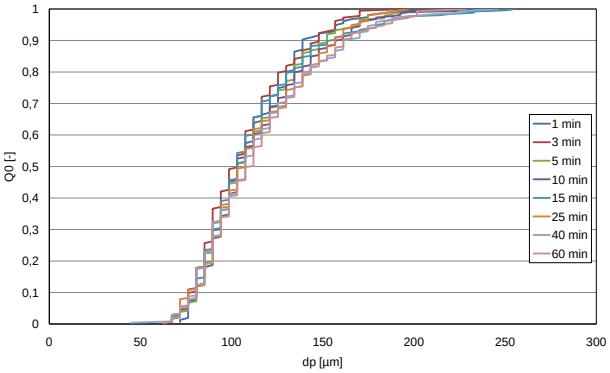

Fig. A9: Roth silicone oil M3 results at 475 from 700 rpm

Also the SFT values have been measured with the device below.

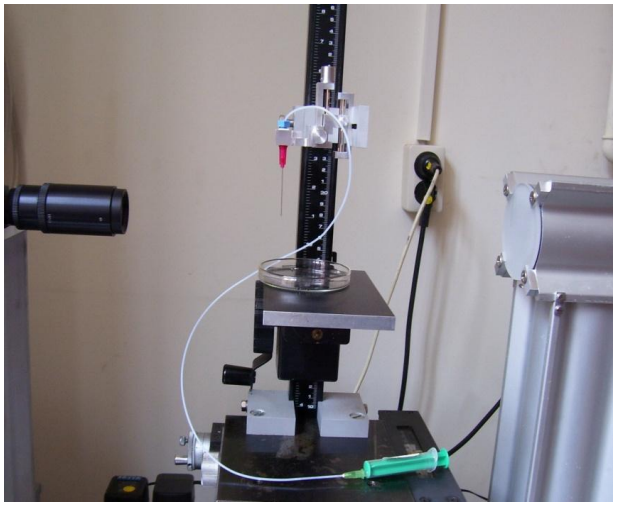

Fig. A10: SFT and IFT measurement device

Tab. A4 Measured SFT values

	Roth silicon oil M3	**Wacker Silicones dimethicone**	**Fauth paraffin oil FC1013**	**Fauth paraffin oil FC1013**	**Fauth paraffin oil FC2006**	**Mobil velocite oil 3 system**
ch.no.	47915003	OM24819	Sample Fauth 31.03.2010	1300038	Sample Fauth 31.03.2010	J0103200
σ [mN/m] measured values	19	16	19	19	53	25

The closer value to the toluene one (σ= 26,6 mN/m) is reported for Mobil velocite oil3.

Additionally has to be said that during the SFT measurements, σ for water was around 67 mN/m instead of the literature value of 72mN/m. Measurements were repeated and gave the same results; which led to the conclusion that SFT values can not be really considered as reliable.

For IFT experience the correctly SFT value for water was verified, due to a deeply cleaning of the device and to great attention to the temperature.

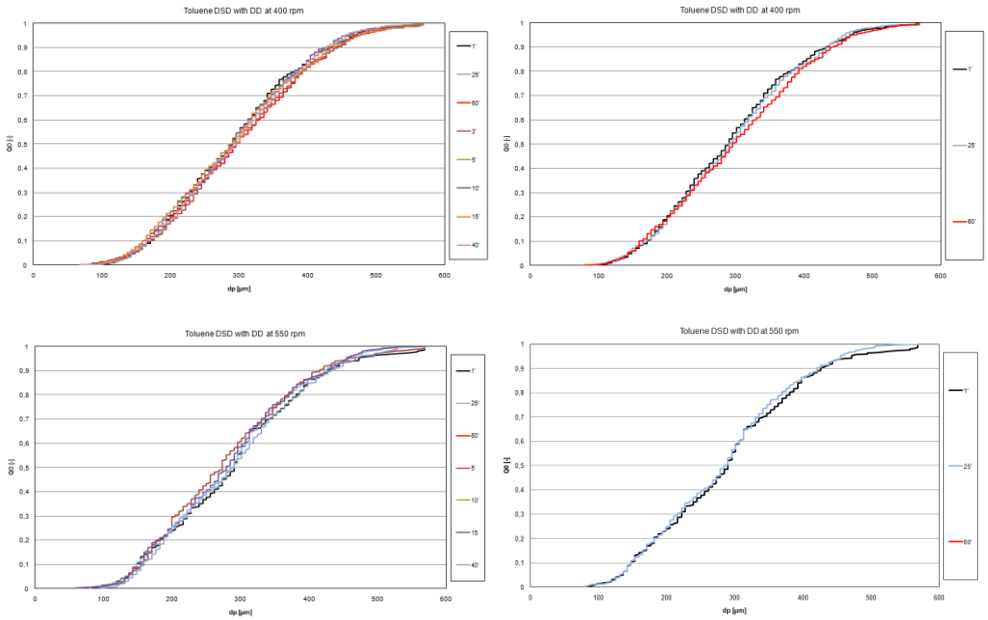

Fig. A11.: Toluene DD results.

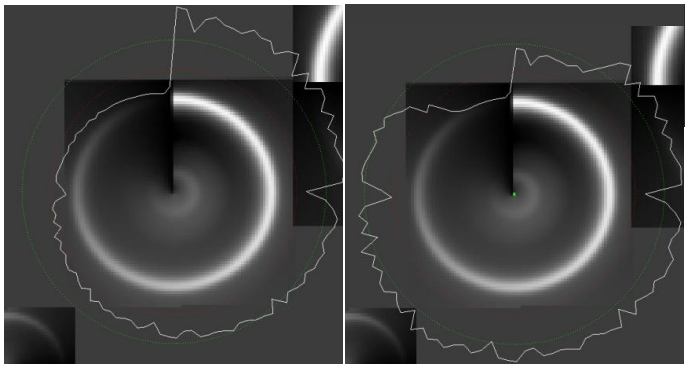

Border property compliance for each angle (a)

Intensity invariant border property compliance for each angle (b)

Fig. A12.: Drop classification (Maaβ et al.,2000)